Anti-Hepatitis B Virus Norbisabolane Sesquiterpenoids from *Phyllanthus acidus* and the Establishment of Their Absolute Configurations Using Theoretical Calculations

Jun-Jiang Lv,[†,‡] Shan Yu,[†,‡] Ya-Feng Wang,[§] Dong Wang,[†] Hong-Tao Zhu,[†] Rong-Rong Cheng,[†] Chong-Ren Yang,[†] Min Xu,*,[†] and Ying-Jun Zhang*,[†]

[†]State Key Laboratory of Phytochemistry and Plant Resources in West China, Kunming Institute of Botany, Chinese Academy of Sciences, Kunming 650201, People's Republic of China

[‡]University of Chinese Academy of Sciences, Beijing 100049, People's Republic of China

[§]School of Pharmaceutical Sciences, Zhengzhou University, Zhengzhou 450001, People's Republic of China

S *Supporting Information*

ABSTRACT: Nineteen new highly oxygenated norbisabolane sesquiterpenoids, phyllanthacidoid acid methyl ester (**1**), and C-T (**4−21**), were isolated from *Phyllanthus acidus* Skeels, together with two known ones, phyllanthusols A (**2**) and B (**3**), whose sugar moiety was revised as glucosamine-*N*-acetate, rather than the previously assigned mannosamine-*N*-acetate. Compounds **2** and **3** were renamed respectively as phyllanthacidoids A (**2**) and B (**3**) to avoid confusion. All of the isolates except for **1** are glycosides, whose saccharide moieties possess a pentaoxy cyclohexane (*scyllo* quercitol) connecting with glucosamine-*N*-acetate or glucosyl moieties, which are first examples in natural products. Phyllanthacidoids N−R (**15−19**) with 8*R* configurations and/or 5,8-diketal skeleton, are

unprecedented structures among norbisabolane sesquiterpenoids. Phyllanthacidoids S (**20**) and T (**21**) have the unusual tricyclo [3.1.1.1] oxygen bridge skeleton formed by a diketal system, of which the relative configurations of the aliphatic chain were assigned on the basis of heteronuclear coupling constants. The absolute configurations of compounds (**1−21**) were established by means of calculated electronic circular dichroism (ECD) and coupling constants. Compounds **1−5**, **7−9**, **10**, and **14** displayed potential anti-hepatitis B virus (HBV) activities, with IC$_{50}$ values of 0.8−36 μM against HBV surface antigen (HBsAg) and HBV excreted antigen (HBeAg), and the results indicated that the 5-ketal group and sugar moieties had contributions to the selectivity of HBsAg and HBeAg.
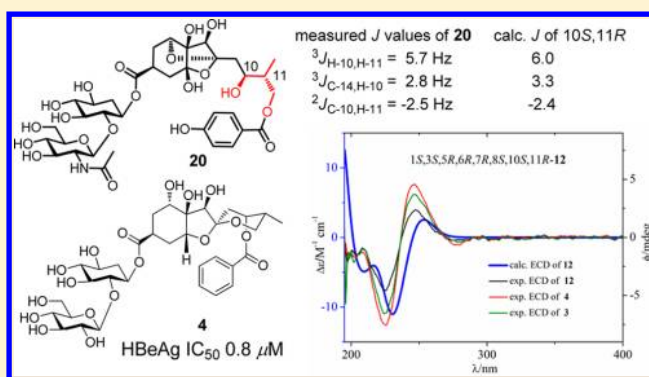
INTRODUCTION

Highly oxygenated bisabolane sesquiterpenoids are mainly found in plants of the *Phyllanthus* genus[1−11] and less frequently in the *Glochidion* genus,[12,13] and most of them exist as glycosides. The first example, phyllanthocin, with strong antileukemic activity, was obtained from *P. brasiliensis* Muell.[1] Phyllaemblicin B, a new norbisabolane glycoside isolated from *P. emblica* Linn by our group previously, showed anticoxsackie virus B3 (CVB3) activity.[10] Structural diversity and potential bioactivities of oxygenated bisabolane sesquiterpenoids have attracted the attention of synthetic chemists.[14]

Phyllanthus acidus Skeels, an important medicinal plant belonging to the genus *Phyllanthus* (Euphorbiaceae), is widely cultivated in Thailand, and its extracts have been used for treating alcoholism.[11] Chemical studies on *P. acidus* in 2000 led to the isolation of two new norbisabolane type sesquiterpenoid glycosides with amino sugars, phyllanthusols A and B.[11] During our research exploring potential antiviral compounds from *Phyllanthus* spp., the methanol extracts of 13 different *Phyllanthus*

species were tested for their antiviral activities against five virus strains: CVB3, hepatitis B virus (HBV), herpes simplex virus type 1 (HSV-1), human enterovirus 71 (EV71), and influenza A (H3N2) virus strain. Among them, the methanolic extract of *P. acidus* displayed potential inhibitory activity against hepatitis B virus HBsAg and HBeAg, with IC$_{50}$ values of 38.6 and 39.0 μg mL^{-1}, respectively. Bioassay-directed isolation of this extract resulted in the purification of 19 new norbisabolane sesquiterpenoid glycosides, phyllanthacidoid acid methyl ester (**1**), and C-T (**4−21**), together with two known ones, phyllanthusols A (**2**) and B (**3**). Their structures were elucidated on the basis of detailed spectroscopic analysis and chemical methods. Structural revisions have been made for the known compounds **2** and **3**, whose sugar moiety should be glucosamine-*N*-acetate, rather than mannosamine-*N*-acetate. Phyllanthacidoids (**1−21**) possess various degree of oxygenation, and phyllanthacidoids

S (**20**) and T (**21**) have an unusual tricyclo [3.1.1.1] oxygen bridge skeleton formed by a diketal system. The relative configurations of the aliphatic chains in **20** and **21** were assigned by measuring heteronuclear coupling constants. Moreover, phyllanthacidoids N−R (**15**−**19**) having the 8R stereochemistry, differ from other norbisabolane sesquiterpenoids. The absolute configurations (Abs) of the norbisabolane sesquiterpenoids **1**−**21** were determined for the first time, by means of calculated ECD using time-dependent density functional theory (TDDFT) and calculated coupling constants. Compounds **1**−**4**, **7**−**9**, **10** and **14** were evaluated for their antiviral activity against HBV, and the results obtained are discussed herein.

■ RESULTS AND DISCUSSION

Air-dried and ground bark and roots of *P. acidus* were extracted with methanol under reflux. After removal of the solvent, the methanol extract showed inhibitory activities against HBsAg and HBeAg secretion, with IC_{50} values of 38.6 and 39.0 μg mL^{-1}, respectively. It was chromatographed over DIAION HP-20SS column to yield five fractions (Fr.1−Fr.5), of which only Fr.2 displayed inhibitory activities against HBsAg (IC_{50} 31.0 μg mL^{-1}) and HBeAg (IC_{50} 28.7 μg mL^{-1}). Further purification of Fr.2 using various chromatographic techniques resulted in the isolation of 21 norbisabolane type sesquiterpenoids, **1**−**21**.
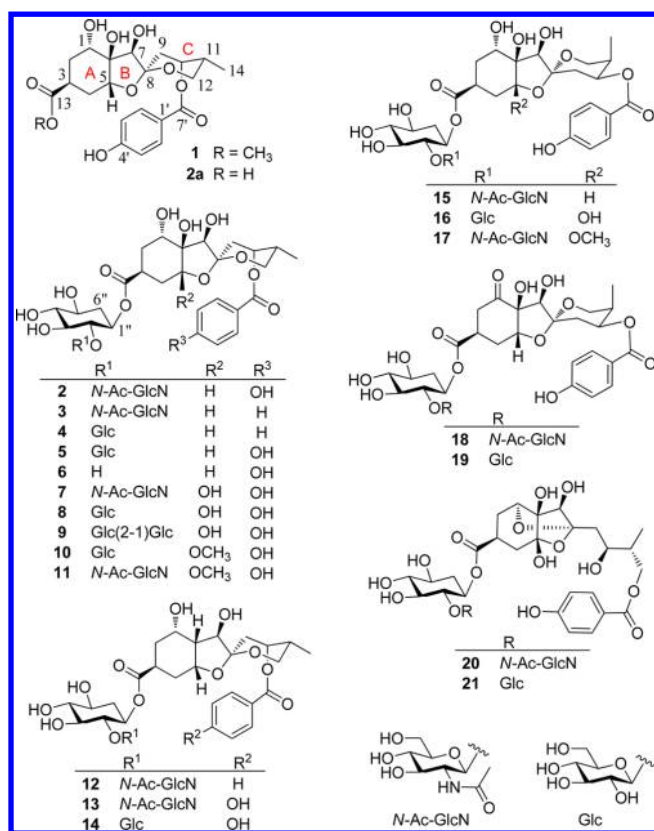
Phyllanthacidoid acid methyl ester (**1**) was obtained as a white amorphous powder with a molecular formula of $C_{22}H_{28}O_{10}$, determined by HRESIMS m/z 451.1621 [M − H]$^-$ (calcd for $C_{22}H_{27}O_{10}$, 451.1610). The ^{1}H NMR spectrum of **1** showed the existence of a *para* substituted benzoyl group [δ_H 6.81 and 7.95 (each 2H, d, $J = 9.0$ Hz)] and a methyl group at δ_H 0.88 (3H, d, $J = 7.2$ Hz). In the ^{13}C NMR and DEPT spectra, besides the signals arising from a benzoyl [δ_C 123.3, 133.1 (2C), 116.2 (2C), 164.0, and 168.2) and a methoxyl (δ_C 52.5) group, 14 carbon

signals including three oxygenated quaternary carbons (one ketal carbon at δ_C 102.6 and one carboxyl carbon at δ_C 178.1), six methines (four oxymethines at δ_C 72.2, 82.2, 76.2 and 71.7), four methylenes (one oxymethylene at δ_C 63.3), and one methyl (δ_C 13.2) were observed, and three ring systems in **1** were deduced from the molecular formula. The aforementioned data indicated that **1** possessed a norbisabolane type sesquiterpenoid skeleton.[11] Its NMR data (Tables 1 and 2) were close to those of the aglycon of phyllanthusol A,[11] except for an additional methoxyl group (δ_C 52.5, δ_H 3.61). Signal of the methoxy (δ_H 3.61) group was correlated with the carboxyl carbon at δ_C 178.1 (C-13) in the HMBC spectrum, which revealed a methyl ester at C-13. Thus, the planar structure of **1** was constructed as shown in Figure 1. The relative configuration was established on the basis of coupling constant analysis and ROESY correlations. The $J_{H-1,H-2}$ (10.5 Hz), $J_{H-3,H-4}$ (11.5 Hz), and $J_{H-5,H-4}$ (3.4 Hz) suggested the axial orientations of H-1 and H-3, and equatorial orientation of H-5. The ROESY correlations of H-1 with H-2eq (δ_H 1.94) and H-4ax (δ_H 1.83), H-3 with H-2ax and H-4eq indicated the opposite face of H-1 (β-orientation) and H-3 (α-orientation). Taking into account of both the axial orientation of H-1 and H-3, it can be proposed that ring A had a boat conformation, and the equatorial H-5 should be α-orientated. The large $J_{H-12,H-11}$ 11.5 Hz showed the axial oriented H-11. Combined with the broad singlet of H-10, it allowed the assignment of H-10 as equatorial, on the same face as H-11. Together with the ROESY correlations of H-7 with H-9, H-2ax and H-3, the relative configuration of compound **1** was established as shown in Figure 1. Compound **1** was likely to be the methanolysis product of the main constituent **2**, formed during the extraction process with methanol under reflux.

Phyllanthacidoids A and B (**2**−**3**), two of the major components, were obtained in yields of 10.3 and 1.0 g from 469 g methanol extract, respectively. The HRESIMS analysis indicated their molecular formulas as $C_{35}H_{49}O_{19}N$ (**2**) and $C_{35}H_{49}O_{18}N$ (**3**), respectively. Comparisons of the ^{13}C NMR and DEPT spectra of compound **2** with those of **1** suggested that the aglycon of **2** shared the same skeleton with **1**, except for the disappearance of the methoxyl carbon (δ_C 52.5), and the appearance of two additional sets of signals from a saccharide unit consisting of seven oxygen bearing methines, one nitrogen bearing methine (δ_C 58.5), one anomeric methine (δ_C 103.1), one oxymethylene, and an acetyl group (Table 1 and Figure S10 in the Supporting Information). On the basis of the HMBC correlation from δ_H 4.71 (H-1″) to the carboxyl carbon C-13 of the aglycon, the HSQC, ^{1}H−^{1}H COSY and QC-TOCSY correlations allowed the construction of the proton spin system of H-1″/H-2″/H-3″/H-4″/H-5″/H-6″/H-1″, attributed to a pentaoxy cyclohexane unit, which was linked to C-13 through an ester bond. The coupling pattern and large J values of H-6ax″ (q, 12.0 Hz) indicated that both H-1″ and H-5″ were axially oriented and on the same face. The J values of H-2″ (dd, 9.2, 9.2 Hz) and H-4″ (dd, 9.2, 9.2 Hz) suggested the axial orientations of H-3″, H-4″ and H-5″. Thus, the pentaoxy cyclohexane group in the saccharide part of **2** was determined to be a substituted *scyllo* quercitol. Furthermore, detailed analysis of HSQC, QC-TOCSY and ^{1}H−^{1}H COSY spectroscopic data of **2** (Figure 2) allowed the construction of another proton spin system, the anomeric proton H-1‴ (δ_H 4.61) with H-2‴/H-3‴/H-4‴/H-5‴/H-6a‴, as a hexosyl unit. The upfield chemical shift δ_C 58.5 of C-2‴ indicated an amino substitution in this position, and the HMBC correlations from H-2‴ and an acetyl methyl H-2⁗ to the acetyl carboxyl carbon at δ_C 174.7 (C-1⁗) revealed that the amino group was acetylated.

Table 1. ^{13}C NMR Spectroscopic Data for Compounds 1−5 in CD_3OD, 6 in DMSO-d_6 (δ in ppm)

no.	1[b]	2[a]	3[a]	4[b]	5[c]	6[c]
1	72.2, CH	72.2, CH	72.3, CH	72.3, CH	72.3, CH	70.4, CH
2	29.3, CH_2	29.2, CH_2	29.5, CH_2	29.0, CH_2	28.6, CH_2	28.4, CH_2
3	34.4, CH	34.8, CH	34.9, CH	34.6, CH	34.3, CH	33.1, CH
4	28.0, CH_2	28.4, CH_2	28.4, CH_2	28.4, CH_2	28.8, CH_2	26.5, CH_2
5	82.2, CH	82.2, CH	82.2, CH	82.4, CH	82.2, CH	79.9, CH
6	76.8, C	76.7, C	76.7, C	76.7, C	76.5, C	74.9, C
7	76.2, CH	76.2, CH	76.4, CH	76.3, CH	76.0, CH	74.6, CH
8	102.6, C	102.6, C	102.7, C	102.6, C	102.6, C	101.0, C
9	36.2, CH_2	36.3, CH_2	36.3, CH_2	36.2, CH_2	35.8, CH_2	35.1, CH_2
10	71.7, CH	71.6, CH	72.2, CH	72.3, CH	71.6, CH	69.8, CH
11	34.4, CH	34.3, CH	34.3, CH	34.3, CH	34.5, CH	32.6, CH
12	63.3, CH_2	63.3, CH_2	63.3, CH_2	63.3, CH_2	63.3, CH_2	61.4, CH_2
13	178.1, C	176.9, C	176.8, C	176.9, C	177.1, C	175.5, C
14	13.2, CH_3	13.2, CH_3	13.2, CH_3	13.2, CH_3	13.2, CH_3	12.8, CH_3
1′	123.3, C	123.3, C	132.4, CH	132.5, CH	123.4, CH	121.6, CH
2′,6′	133.1, CH	133.4, CH	131.0, CH	131.0, CH	133.5, CH	131.9, CH
3′,5′	116.2, CH	116.3, CH	129.8, CH	129.7, CH	116.5, CH	115.3, CH
4′	164.0, C	163.6, C	134.4, CH	134.3, CH	163.6, C	162.1, C
7′	168.2, C	168.4, C	168.2, C	168.0, C	168.4, C	166.1, C
1′		70.6, CH	70.5, CH	70.6, CH	70.5, CH	71.6, CH
2″		83.3, CH	82.9, CH	85.8, CH	86.7, CH	74.6, CH
3″		76.7, CH	76.8, CH	76.1, CH	76.0, CH	74.7, CH
4″		78.6, CH	78.8, CH	78.3, CH	78.1, CH	77.1, CH
5″		69.7, CH	69.8, CH	69.9, CH	69.9, CH	68.3, CH
6″		35.9, CH_2	36.1, CH_2	35.8, CH_2	36.4, CH_2	35.0, CH_2
1‴		103.1, CH	102.8, CH	105.9, CH	106.5, CH	
2‴		58.5, CH	58.4, CH	76.0, CH	76.2, CH	
3‴		76.9, CH	77.0, CH	77.9, CH	78.0, CH	
4‴		71.9, CH	71.8, CH	71.0, CH	70.7, CH	
5‴		77.9, CH_2	77.9, CH_2	77.8, CH_2	77.8, CH_2	
6‴		62.6, CH_2	62.6, CH_2	62.4, CH_2	62.2, CH_2	
1⁗		174.7, C	174.6, C			
2⁗		23.2, CH_3	23.2, CH_3			
OCH_3	52.5, CH_3					

[a,b,c]Data were recorded at 100, 125 and 150 MHz, respectively.

The large coupling constants of $J_{H-1‴,\ H-2‴}$ (8.3 Hz), $J_{H-2‴,\ H-3‴}$ (9.8 Hz), $J_{H-3‴,\ H-4‴}$ (8.8 Hz) and $J_{H-4‴,\ H-5‴}$ (8.8 Hz) indicated the axial orientations for all of these five protons in the sugar unit, which was further confirmed by the ROESY correlations of H-1‴ with H-3‴ and H-5‴, H-2‴ with H-4‴, and H-4‴ with H-6‴. Thus, the signals from the sugar moiety in **2** were assigned as 2-acetamido-2-deoxy-β-glucopyranose. The HMBC correlation from H-1‴ to δ_C 83.3 (C-2″) allowed the construction of the saccharide moiety in **2** as *scyllo* quercitol-2-*O*-β-glucosamine-*N*-acetate.

The NMR data of compound **3** were close to those of **2**, except that the benzoyl moiety replaced the *p*-hydroxyl benzoyl group in **2** (Figure 2). The structural features of **2** and **3** were similar to those of phyllanthusols A and B, respectively, reported by Vongvanich et al. in 2000 as the major chemical constituents from the titled plant.[11] The ^{13}C NMR data of **2** and **3** were plotted against the reported data[11] of phyllanthusol A and B (ph-A and B), respectively, and the least-squares values of correlation factors (R^2) were determined (0.99979 for **2**, and 0.99998 for **3**). The difference plots in Figure 3 were determined by subtracting the chemical shifts of ph-A and B from those of **2** and **3**, respectively. For **2** and ph-A, the average deviation $|\Delta\delta|$ was 0.4 ppm, and only C-1′ and C-6′ of the *p*-hydroxylbenzoyl group showed differences between 1.8 and 2.7 ppm. Although it is difficult to explain the differences, it is sure that there is no structure alternation for the *p*-hydroxylbenzoyl fragment in both **2** and ph-A based on 2D NMR experiments. In the case of compound **3** and ph-B, the average deviation $|\Delta\delta|$ was 0.3 ppm, and the average deviation $|\Delta\delta|$ for each carbon was smaller than 0.6 ppm. Therefore, taking into account of the above statistical data, the 2D NMR data (Figure S11−15 in Supporting Information), and the same biological source, it is obvious that **2** and ph-A, **3** and ph-B have the same structures, respectively.

The saccharide moiety in phyllanthacidoid A = phyllanthusol A was determined to be *scyllo* quercitol-2-*O*-α-mannosamine-*N*-acetate by Vongvanich et al.,[11] in which most *J* values of the amino sugar moiety were not reported, except for $J_{H-1″,H-2‴}$, maybe because of the lower resolution of 400 MHz NMR spectrometer. However, the large value of $J_{H-3‴,\ H-4″}$ (8.8 Hz) observed in the ^1H NMR spectrum of **2** did not support the existence of α-mannosamine-*N*-acetate in **2**. Thus, the saccharide moiety of phyllanthusol A should be revised as *scyllo* quercitol-2-*O*-β-glucosamine-*N*-acetate. Compound **2** was subsequently hydrolyzed by an aqueous solution of NaOH (0.1 M) to yield the aglycon, which was named as phyllanthacidoid acid (**2a**), and a saccharide residue, which was established as *scyllo* quercitol-2-*O*-β-glucosamine-*N*-acetate by detailed analysis of the ^1H and ^{13}C NMR, HSQC, QC-TOCSY and ^1H−^1H COSY experiments
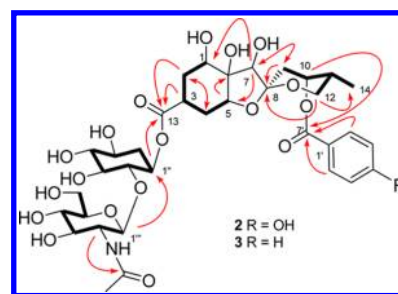
Table 2. ^{1}H NMR Spectroscopic Data for Compounds 1−5 in CD$_3$OD and 6 in DMSO-d_6 (δ in ppm)

no.	1^a	2^b	3^b	4^a	5^b	6^b
1	3.78 dd (4.8, 10.5)	3.85 dd (5.3, 10.5)	3.86 dd (5.4, 10.4)	3.83 dd (5.5, 10.5)	3.83 dd (5.5, 10.6)	3.62 dd (4.2, 9.7)
2	1.55 ddd (9.5, 10.5, 14.2)	1.63 ddd (9.4, 10.3, 14.3)	1.67 ddd (14.0, 9.1, 10.3)	1.60 ddd (14.0, 9.1, 10.5)	1.56 ddd (9.3, 10.5, 14.2)	1.48 ddd (14.0, 9.3, 9.7) 1.74^c
	1.94 ddd (14.2, 5.4, 5.4)	2.10^c	2.11^c	2.11^c	2.12^c	
3	2.51 m	2.57 m	2.56 m	2.59 m	2.58 m	2.43 ddt (8.7, 6.0, 11.4)
4	1.83 ddd (3.4, 11.5, 14.5)	1.92 dd (3.6, 8.6)	1.86 dt (14.6, 4.7)	1.85 ddd (3.0, 12.0, 15.0)	1.82 ddd (3.0, 12.8, 14.6)	1.74^c
	1.94 m		1.96 ddd (4.1, 12.3, 14.6)	1.93 ddd (3.5, 5.5, 15.0)	2.01 m	1.82^c
5	4.02 t (3.4)	4.08 t (3.5)	4.10 t (3.5)	4.10 t (3.0)	4.09 brs	3.89 t (3.6)
7	3.78 s	3.81 s	3.85 s	3.81 s	3.81 s	3.66 s
9	2.11 m	2.12^c	2.16^c	2.10 m	2.11 m	1.88 m
						2.04 m
10	5.20 brs	5.23 brs	5.28 brs	5.27 brs	5.23 brs	5.13 brs
11	2.10 m	2.10^c	2.13^c	2.12 m	2.11^c	2.00 m
12	3.58 dd (4.0, 11.5)	4.04 dd (11.4, 11.4)	4.07 dd (11.7, 11.7)	3.63^c	3.62 dd (1.6, 11.6) 4.06 dd (11.6, 11.6)	3.50^c
	4.00 dd (11.5, 11.5)	3.59^c	3.36 dd (11.7, 4.6)	4.05 dd (11.4, 11.4)		3.84 dd (11.4, 11.4)
14	0.88 d (7.2)	0.89 d (7.2)	0.90 d (6.9)	0.89 d (6.9)	0.89 d (7.0)	0.77 d (7.2)
2′,6′	7.95 d (9.0)	7.99 d (8.7)	8.12 d (8.4)	8.14 d (8.0)	8.02 d (8.8)	7.89 d (7.8)
3′,5′	6.81 d (9.0)	6.86 d (8.7)	7.50 t (7.8)	7.52 t (8.0)	6.88 d (8.8)	6.82 d (7.8)
4′			7.63 brt (7.5)	7.66 brt (7.4)		
1″		4.71 ddd (5.0, 9.8, 12.0)	4.69^c	4.73 m	4.75 ddd (4.9, 9.5, 12.0)	4.50 ddd (4.5, 9.5, 12.0)
2″		3.60 dd (9.2, 9.2)	3.57 dd (9.3, 9.3)	3.37^c	3.45 dd (9.5, 9.5)	3.15 dd (9.5, 9.5)
3″		3.30 m	3.29 dd (9.3, 9.3)	3.31 dd (9.2, 9.2)	3.36 dd (9.5, 9.5)	2.98 dd (9.5, 9.5)
4″		3.24 dd (9.2, 9.2)	3.18 dd (9.3, 9.3)	3.24 dd (9.2,9.2)	3.32^c	3.02^c
5″		3.43 ddd (4.3, 9.2, 12.0)	3.42 m	3.43 ddd (4.5, 9.2, 12.0)	3.46 m	3.27 ddd (4.5, 8.7, 12.0)
6″		1.42 q (12.0)	1.34 q (12.0)	1.35 q (12.0)	1.47 q (12.0)	1.30 q (2.0)
		2.06 m	2.17 m	2.04^c	2.10 m	1.89 m
1‴		4.61 d (8.3)	4.51 d (8.3)	4.23 d (8.0)	4.16 d (8.0)	
2‴		3.50 dd (8.3, 9.8)	3.52 dd (8.3, 9.7)	3.12 dd (8.0, 9.0)	3.12 dd (8.0, 9.0)	
3‴		3.39 dd (8.8, 9.8)	3.39 dd (8.8, 9.7)	3.30^c	3.32 dd (9.0, 9.0)	
4‴		3.26 dd (8.8, 8.8)	3.35 dd (8.8, 8.8)	3.28 dd (9.0, 9.0)	3.36^c	
5‴		2.98 ddd (2.4, 4.3, 8.8)	3.03 ddd (2.9, 4.6, 8.8)	2.87 ddd (2.5, 3.5, 9.0)	2.78 ddd (2.5, 4.0, 8.0)	
6‴		3.62 dd (2.4, 11.8)	3.66 m	3.59 m	3.46 m	
		3.65 dd (4.5, 11.8)			3.58 dd (4.3, 11.0)	
2⁗		2.01 s	2.00 s			
OCH$_3$	3.61 s					

^{a,b}Data were recorded at 500 and 600 MHz, respectively. ^{c}Signals were overlapped with each other or by solvents.
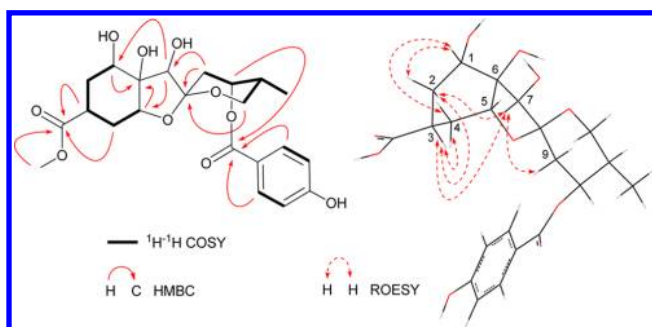
Figure 1. Key ^{1}H−^{1}H COSY, HMBC and ROESY correlations of **1**.

Figure 2. Key ^{1}H−^{1}H COSY (—) and HMBC (→) correlations of **2** and **3**.

(Figure S169−174 in Supporting Information). In turn, **2** was hydrolyzed by an aqueous solution of HCl (3 M) at 80 °C to afford *scyllo* quercitol and glucosamine. The positive $[\alpha]^{25}_D$ +10.6 (*c* 0.2, MeOH) of glucosamine indicated its D configuration. For *scyllo* quercitol, the tested $[\alpha]^{25}_D$ was −16.5 (*c* 5.5, MeOH). However, there is no available literature to report

the absolute configuration of *scyllo* quercitol, because of the rare occurrence of this compound in nature. The TDDFT/GIAO method was applied to calculate the optical rotations of two enantiomers of *scyllo* quercitol, and the calculated $[\alpha]_D$ values of 1R,2S,4R,5S- and 1S,2R,4S,5R- *scyllo* quercitol were 16.3 and −17.4, respectively. Therefore, the absolute configuration of *scyllo* quercitol in **2** was determined as 1S,2R,4S,5R. In
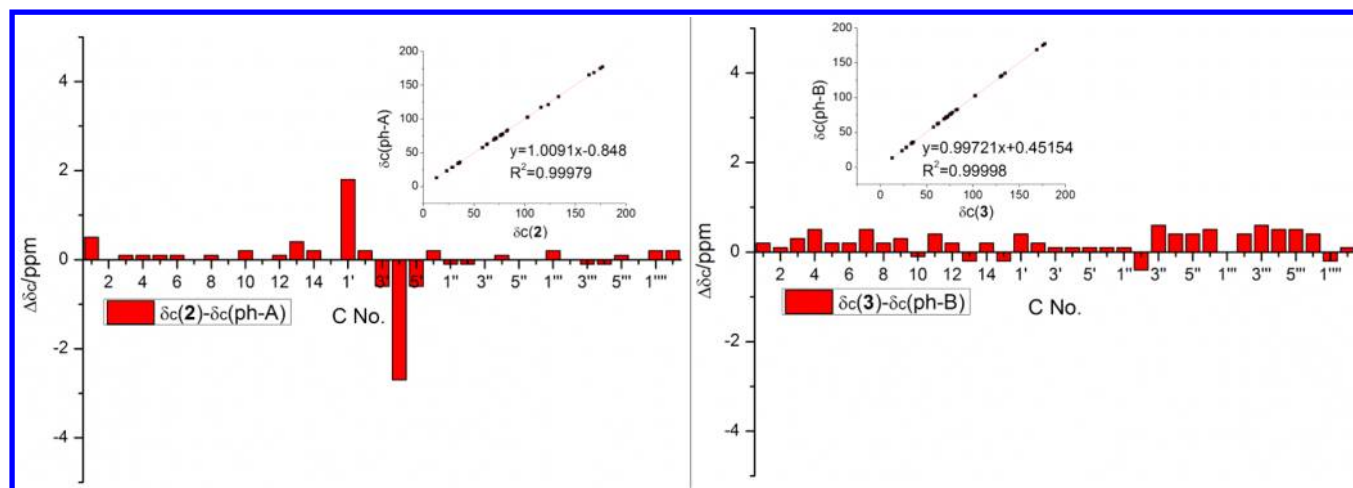
Figure 3. ^{13}C chemical shifts difference plots of **2** and **3** with ph-A and B, respectively. The δ_C data were measured at the same NMR conditions as the literature, i.e., the solvents of D_2O/CD_3OD 1:2.

conclusion, the structures of phyllanthusols A and B were revised and renamed as phyllanthacidoids A (**2**) and B (**3**), respectively, e.g., phyllanthusol A = phyllanthacidoid A and phyllanthusol B = phyllanthacidoid B.

The molecular formulas of phyllanthacidoids C–E (**4**–**6**) were assigned to be $C_{33}H_{46}O_{18}$, $C_{33}H_{46}O_{19}$, and $C_{27}H_{36}O_{14}$, respectively, on the basis of HRESIMS. Analysis of their NMR data (Tables 1 and 2) revealed that all of them had the same norbisabolane part of the aglycons as phyllanthacidoids A–B (**2**–**3**). The main difference between the NMR spectra of **4** and **3** was the disappearance of the N-substituted methine at δ_C 58.4 (C-2‴) and the signals of the acetyl group, while the signals from a typical β-glucosyl unit were observed in the NMR spectra (Table 1) of **4**. The pentaoxy cyclohexane moiety was determined to be *scyllo* quercitol on the basis of the coupling constant analysis and ^1H–^1H COSY correlations. For the glucosyl moiety, the signals were assigned according to the ^1H–^1H COSY, HSQC and HMBC correlations (Figure S31–34 in Supporting Information). The axial orientations of all the glucosyl protons were determined by the large J values ($J_{H-1''}$= 8.0 Hz, $J_{H-2''}$= 8.0, 9.0 Hz, and $J_{H-4''}$= 9.0, 9.0 Hz). Connectivity of the sugar part was confirmed by the HMBC correlations from H-1″ to C-13, and H-2‴ to C-2″. Compound **4** was hydrolyzed to afford *scyllo* quercitol and glucose $[\alpha]_D^{25}$ +26.6 (c 0.6, MeOH). The above data indicated that the saccharide unit of **4** was *scyllo* quercitol-2-*O*-β-D-glucose. Compound **5** had the same aglycon as **2**, and its saccharide moiety was determined to be *scyllo* quercitol-2-*O*-β-glucose too, by 2D NMR. The NMR spectroscopic data of **6** were comparable to those of **2**, except for the absence of the signals from β-glucosamine-*N*-acetate unit. 2D NMR experiments confirmed that **6** was a derivative of **2** lacking of a β-glucosamine-*N*-acetate unit.

Phyllanthacidoid F (**7**) had a molecular formula $C_{35}H_{49}NO_{20}$, as deduced from its HRESIMS. Comparison of the NMR data (Tables 3 and 4) with those of **2** revealed a change of the oxymethine group C-5, and a ketal carbon (δ_C 105.2) replaced the methine (δ_C 82.2) in **2**. This was supported by the ^1H–^1H COSY correlations of H-1/H-2/H-3/H-4 and the HMBC correlations from H-1, H-3 and H-7 to C-5 (Figure 4). The J values of H-1 (dd, J = 5.5, 9.0 Hz) revealed its axial orientation, which was supported by the ROESY correlations of H-1 with H-2eq (δ_H 2.18) and H-4ax (δ_H 1.86). The large $J_{H-3,H-2}$ value (9.5 Hz) indicated the axial orientation of H-3, and the ROESY

Table 3. ^{13}C NMR Spectroscopic Data for Compounds **7**–**11** in CD_3OD (δ in ppm)

no.	7[b]	8[a]	9[a]	10[b]	11[c]
1	72.0, CH	72.1, CH	71.9, CH	71.9, CH	71.9, CH
2	29.7, CH$_2$	29.0, CH$_2$	28.8, CH$_2$	31.0, CH$_2$	31.4, CH$_2$
3	35.4, CH	35.2, CH	35.1, CH	35.0, CH	35.0, CH
4	36.3, CH$_2$	36.5, CH$_2$	36.5, CH$_2$	32.3, CH$_2$	31.8, CH$_2$
5	105.2, C	105.1, C	104.9, C	106.8, C	106.8, C
6	78.1, C	78.0, C	78.0, C	78.6, C	78.6, C
7	76.1, CH	75.9, CH	75.9, CH	77.7, CH	77.9, CH
8	102.8, C	102.9, C	102.8, C	103.8, C	103.8, C
9	36.3, CH$_2$	36.6, CH$_2$	36.5, CH$_2$	37.1, CH$_2$	36.9, CH$_2$
10	71.7, CH	71.7, CH	71.5, CH	71.7, CH	71.6, CH
11	34.2, CH	34.2, CH	34.0, CH	34.2, CH	34.3, CH
12	63.9, CH$_2$	64.0, CH$_2$	63.9, CH$_2$	64.8, CH$_2$	64.8, CH$_2$
13	176.2, C	176.2, C	176.9, C	176.4, C	176.2, C
14	13.2, CH$_3$	13.2, CH$_3$	13.1, CH$_3$	13.2, CH$_3$	13.3, CH$_3$
1′	123.2, CH	123.5, CH	123.3, CH	123.4, CH	123.2,CH
2′,6′	133.6, CH	133.7, CH	133.7, CH	133.3, CH	133.2,CH
3′,5′	116.3, CH	116.4, CH	116.4, CH	116.5, CH	116.4,CH
4′	163.5, C	163.4, C	163.3, C	163.5, C	163.8, C
7′	168.4, C	168.3, C	168.0, C	168.1, C	168.2, C
1″	70.9, CH	70.9, CH	70.8, CH	70.7, CH	70.5, CH
2″	83.6, CH	86.3, CH	86.9 CH	85.7, CH	83.0, CH
3″	76.5, CH	75.9, CH	75.4, CH	76.2, CH	77.0, CH
4″	78.6, CH	78.0, CH	77.1, CH	78.2, CH	78.9, CH
5″	69.8, CH	70.0, CH	69.7, CH	69.9, CH	69.8, CH
6″	35.8, CH$_2$	35.6, CH$_2$	35.5, CH$_2$	35.8, CH$_2$	35.9, CH$_2$
1‴	103.2, CH	106.5, CH	104.6, CH	105.9, CH	102.9,CH
2‴	58.6, CH	76.4, CH	85.3, CH	76.3, CH	58.5, CH
3‴	76.8, CH	77.9, CH	77.6, CH	78.1, CH	77.0, CH
4‴	71.7, CH	71.1, CH	70.5, CH	71.2, CH	71.7, CH
5‴	77.9, CH$_2$	78.1, CH$_2$	77.4, CH	77.7, CH$_2$	77.9, CH$_2$
6‴	62.7, CH$_2$	62.5, CH$_2$	62.1, CH$_2$	62.5, CH$_2$	62.6, CH$_2$
1⁗	174.9, C		106.4 CH		174.7, C
2⁗	23.3, CH$_3$		76.4 CH		23.2, CH$_3$
3⁗			78.8 CH		
4⁗			70.9 CH		
5⁗			77.8 CH		
6⁗			62.3 CH$_2$		
OCH$_3$				49.0, CH$_3$	50.0, CH$_3$

^{a,b,c}Data were recorded at 100, 125 and 150 MHz, respectively.

Table 4. ^{1}H NMR Spectroscopic Data for Compounds 7−11 in CD$_3$OD (δ in ppm)

no.	7[c]	8[a]	9[d]	10[b]	11[c]
1	3.94 dd (5.5, 9.0)	3.91 dd (6.5, 9.5)	3.91 dd (6.5, 9.0)	3.83 dd (4.0, 5.0)	3.85 dd (3.7, 4.8)
2	1.69 dt (14.5, 9.5)	1.61 m	1.63 dt (14.5, 9.0)	1.89 m	1.94[e]
	2.18 m	2.21 m	2.22 dt (14.5, 6.5)		1.99[e]
3	2.45 m	2.48 m	2.46 m	2.49 tt (5.5, 11.0)	2.46 tt (5.1, 10.7)
4	1.86 dd (11.0, 14.0)	1.74 dd (12.5, 13.0)	1.72 dd (12.5, 13.5)	1.59 dt (11.0, 13.5)	1.70 dd (10.7, 13.7)
	1.94 dd (5.0, 14.0)	2.01 m	2.03 m	2.15 dd (4.5, 13.5)	2.06 m
7	3.87 s	3.85 s	3.85 s	3.88 s	3.89 s
9	2.11 m	2.10 m	2.11[e]	1.95 dd (3.0, 15.0)	1.96 dd (3.3, 15.0)
				2.60 dd (3.0, 15.0)	2.58 dd (2.8, 15.0)
10	5.21 brs	5.21 brs	5.21brs	5.18 brs	5.18 brs
11	2.11 m	2.10 m	2.10 m	2.11 m	2.08[e]
12	3.60 dd (5.0, 11.5)	3.69 m	3.61 m	3.70 dd (5.0, 11.5)	3.71 m
	4.15 dd (11.5,11.5)	4.17 dd (11.5, 11.5)	4.18 dd (11.6, 11.6)	4.18 dd (11.5, 11.5)	4.17 dd (11.7, 11.7)
14	0.89 d (7.0)	0.89 d (6.9)	0.89 d (7.0)	0.90 d (7.0)	0.91 d (7.1)
2′,6′	8.03 d (9.0)	8.07 d (8.5)	8.08 d (8.5)	8.00 d (9.0)	8.00 d (9.0)
3′,5′	6.87 d (9.0)	6.90 d (8.5)	6.91 d (8.5)	6.85 d (9.0)	6.85 d (9.0)
1″	4.65 ddd (4.9, 9.6, 12.0)	4.69 ddd (4.9, 9.2, 12.0)	4.68 ddd (4.9, 9.5, 12.0)	4.72 ddd (4.8, 9.5, 12.0)	4.67 ddd (4.8, 9.5, 12.1)
2″	3.48 dd (9.6, 9.6)	3.32[e]	3.23 (9.5, 9.5)	3.45 dd (9.5, 9.5)	3.59 dd (9.5, 9.5)
3″	3.28 dd (9.3, 9.3)	3.33[e]	3.46 dd (9.5, 9.5)	3.34 dd (9.5, 9.5)	3.29[e]
4″	3.25 dd (9.3, 9.3)	3.26 dd (9.6, 9.6)	3.35[e]	3.32[e]	3.23 dd (9.3, 9.3)
5″	3.42 m	3.44 m	3.49 m	3.45 m	3.44 m
6″	1.34 q (12.0)	1.36 q (12.0)	1.35 q (12.0)	1.43 q (12.0)	1.40 q (12.1)
	2.06 m	2.02 m	2.10 m	2.05 m	2.07[e]
1‴	4.56 d (8.5)	4.11 d (8.0)	4.18 d (8.3)	4.25 d (8.0)	4.66 d (8.4)
2‴	3.51 dd (8.5, 9.5)	3.13 dd (8.0, 9.1)	3.33[e]	3.12 dd (8.0, 9.0)	3.49 dd (8.4, 10.1)
3‴	3.43[e]	3.40 dd (9.1, 9.1)	3.61 dd (9.4, 9.4)	3.32 m	3.41[e]
4‴	3.37 dd (9.2, 9.2)	3.27[e]	3.35[e]	3.25 dd (9.5, 9.5)	3.32[e]
5‴	3.04 m	2.98 ddd (3.4, 3.4, 9.6)	2.88 dt (9.8, 2.9)	2.98 m	3.07 ddd (2.4, 5.7, 9.7)
6‴	3.68 m	3.60 m	3.46 m	3.61 dd (4.5, 12.0)	3.69 m
			3.61 m	3.65 dd (2.5, 12.0)	
1⁗			4.62 d (8.0)		
2⁗	2.01 s		3.33 dd (8.0, 9.0)		2.00 s
3⁗			3.39 dd (9.0, 9.0)		
4⁗			3.37 dd (9.0, 9.0)		
5⁗			3.38 ddd (2.1, 4.7, 9.0)		
6⁗			3.73 dd (4.0, 12.0)		
			3.90 brd (12.0)		
OCH$_3$				3.39 s	3.40 s

[a,b,c,d]Data were recorded at 400, 500, 600, and 800 MHz, respectively. [e]Signals were overlapped with each other or by solvents.

correlations of H-3 with H-2ax and H-4eq suggested that it is on the opposite face to H-1. With the above results, it can be concluded that ring A in **7** had a boat conformation like compound **1** (Figure 1). Together with the ROESY correlations of H-7 with H-9, H-2ax and H-3, the relative configuration of the aglycon of **7** was established. Therefore, the structure of **7** was elucidated and named as phyllanthacidoid F, and it is the first example of a 5,8-diketal norbisabolane sesquiterpenoid.

Phyllanthacidoids G (**8**) and H (**9**) possessed molecular formulas of C$_{33}$H$_{46}$O$_{20}$ and C$_{39}$H$_{56}$O$_{25}$, respectively, as established on the basis of HRESIMS. Detailed analysis of their NMR data (Tables 3 and 4) indicated that both compounds shared the same aglycon as **7**, but had different saccharide moieties. The saccharide moiety of **8** was determined as *scyllo* quercitol-2-*O*-β-glucopyranose. In the case of compound **9**, besides the *scyllo* quercitol-2-*O*-β-glucopyranose moiety, an additional hexosyl moiety [anomeric center at δ_C 106.4 (C-1⁗) and δ_H 4.62 (1H, d, J = 8.0 Hz, H-1⁗)] and the HMBC correlation from H-1⁗ to the middle glucosyl C-2‴ was observed in the NMR spectra. The ^{1}H NMR signals due to the sugar units
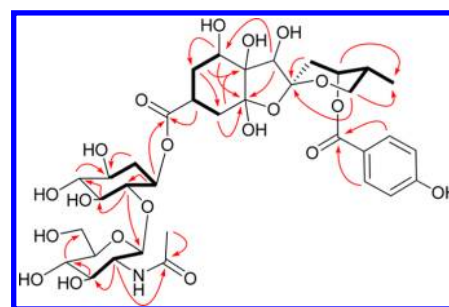
Figure 4. Key ^{1}H−^{1}H COSY (—), and HMBC (→) correlations of **7**.

were heavily overlapped even though recorded on a 500 MHz NMR spectrometer, which made it difficult to distinguish the type of the sugar. When the ^{1}H NMR spectrum was measured on an 800 MHz NMR spectrometer, together with QC-TOCSY technique (Figure S70 in Supporting Information), the signals of the additional hexosyl unit were assignable in **9**. The six carbon signals and their corresponding protons were fully assigned

(Table 4), and this sugar was determined as β-glucose on the basis of the coupling constants.

The molecular formulas of phyllanthacidoids I−J (**10**−**11**) were determined as $C_{34}H_{48}O_{20}$ and $C_{36}H_{51}NO_{20}$, respectively, on the basis of HRESIMS. The molecular weight of **10** was 14 Da more than that of **8**. The NMR features of **10** were close to those of **8**, except for an addition methoxyl signal (δ_C 49.0 and δ_H 3.39) in **10**. Connectivity of the methoxyl group was confirmed by its HMBC correlation from δ_H 3.39 to C-5 (δ_C 106.8), suggesting that **10** was the 5-OH methylated derivative of **8**. The relative configuration of ring C was the same as that of **8**, which was determined by coupling constants. H-1 with small coupling constants (4.0 and 5.0 Hz), was assigned an equatorial orientation. The axial orientation of H-3 (tt, J = 5.5, 11.0 Hz) was determined by its J values. The ROESY correlations of H-1 with H-4ax (δ_H 1.59), and H-3 with H-4eq indicated the opposite face of H-3 to H-1, and showed that ring A had a chair conformation (Figure 5), unlike the boat conformations of **1**−**9**.
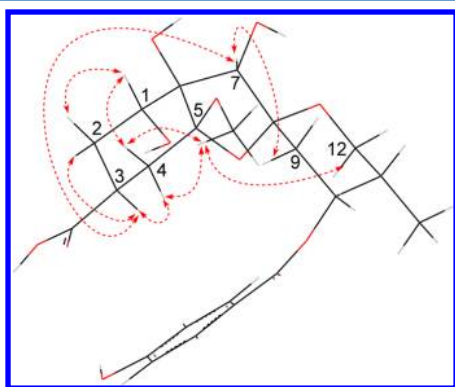

Figure 5. Key ROESY correlations of **10**.

Taking into account of the ROESY correlations of H-7 with H-3 and H-9, 5−OCH₃ with H-12, it allowed the construction of the relative configurations of compound **10** as shown (Figure 5). Both the planar structure and relative configuration of the aglycon of **11** were the same as those of **10**, and the saccharide moiety of **11** was determined to be *scyllo* quercitol-2-*O*-β-glucosamine-*N*-acetate.

The molecular formulas of phyllanthacidoids K-M (**12**−**14**) were determined to be $C_{35}H_{49}NO_{17}$, $C_{35}H_{49}NO_{18}$, and $C_{33}H_{46}O_{18}$, respectively, by HRESIMS, which were one oxygen atom less than those of **3**, **2** and **5**, respectively. The NMR spectra of **12**−**14** were close to those of **3**, **2** and **5**, except that the oxygenated quaternary carbon of C-6 at δ_C 76.7 (**3**), 76.7 (**2**), and 76.5 (**5**) was replaced by an aliphatic methine in **12** (δ_C 47.8), **13** (δ_C 47.9) and **14** (δ_C 48.0), and whose corresponding C-1 signals were upfield shifted by $\Delta\delta$ > 6.0 ppm to δ_C 65.9 (**12**), 66.1 (**13**), and 65.9 (**14**), respectively (Table 5). The aforementioned data indicated that compounds **12**−**14** were the C-6 dehydroxyl analogues of **3**, **2** and **5**, respectively.

In compound **12**, the aliphatic methine signal at δ_C 47.8 was assigned as C-6 on the basis of the ^1H−^1H COSY correlations of H-1/H-6/H-5 and the HMBC correlations from H-6 to C-2 and C-5. The relative configuration of **12** was the same as those of **1**−**9**. On the basis of the same method, the planar structure and relative configurations of **13** and **14** were established. Both **13** and **14** have the same aglycon as that of **12**, except for a *para*-hydroxylated benzoate moiety connected to the 10-OH. The saccharide moieties in compounds **12** and **13** were both

scyllo quercitol 2-*O*-β-glucosamine-*N*-acetate, and in **14** it was *scyllo* quercitol 2-*O*-β-glucopyranose.

Phyllanthacidoid N (**15**) had the same molecular formula $C_{35}H_{49}NO_{19}$ as compound **2**, as established from HRESIMS. The 2D NMR data (Figure 6) revealed that compound **15** had the same planar structure as **2**. However, differences in chemical shifts of δ_C 32.3 (C-2, $\Delta\delta$ +3.1), δ_C 76.9 (C-5, $\Delta\delta$ −5.3), δ_C 90.2 (C-7, $\Delta\delta$ +14.0), δ_C 108.6 (C-8, $\Delta\delta$ +6.0), δ_C 30.4 (C-9, $\Delta\delta$ −5.9), δ_C 66.1 (C-12, $\Delta\delta$ +2.8) were observed in the ^{13}C NMR (Table 6) of **15**, compared with that of **2**. This implied that **15** was a stereoisomer of **2**. The J values of H-3 (tt, 3.5, 12.5 Hz) indicated its axial orientation. The triplet of H-1 (3.2 Hz) and H-5 (3.1 Hz) indicated their equatorial orientation on the opposite face of H-3, which was confirmed by the NOE effects of H-1 and H-5 with H-2a (δ_H 1.88), and H-3 with H-2b. The ring A of **15** was of a chair conformation (Figure 6). The small coupling constants of H-12a (1.2, 11.7 Hz) and H-12b (2.1, 11.7 Hz) showed an equatorial orientation of H-11, while the large J value of H-10 (dt, J = 11.6, 5.1 Hz) suggested its axial orientation, on the same side as H-11. The orientations of H-10 and 11 in **15** were different from those in **1**−**14** and other norbisabolane glycosides of this type with H-10 and 11 equatorially and axially orientated, respectively. Additionally, the ROESY correlations of H-7 with H-2b allowed the construction of the relative configuration of **15** (Figure 6). However, the relative configuration from rings A, B to ring C could not be determined by NOE experiments, and ECD calculation was pursued and discussed below.

Phyllanthacidoid O (**16**), with a molecular formula $C_{33}H_{46}O_{20}$, had the same planar structure as **8**, as confirmed by extensive 2D NMR analysis (Figure S116−119 in Supporting Information). However, compared with **8**, differences of the chemical shifts of C-7 ($\Delta\delta$ 2.9), C-8 ($\Delta\delta$ 5.3), C-9 ($\Delta\delta$ −3.5), C-12 ($\Delta\delta$ 3.0), C-14 ($\Delta\delta$ −2.5) were observed in ^{13}C NMR spectrum of **16** (Table 6), which suggested that **16** was a stereoisomer of **8**. The relative configuration of ring C was assigned to be the same as that of **15**, on the basis of the coupling constant analysis. The J values of H-1 (dd, J = 5.1, 11.4 Hz), and the ROESY correlation with H-2eq (δ_H 2.29), indicated its axial orientation. The signal of H-3 displayed weak ROESY correlations with H-2eq and H-4eq (δ_H 2.44), and strong correlations with H-2ax and H-4ax, indicated its equatorial orientation. Thus, H-1 and H-3 was at the opposite face, and the conformation of ring A was chair (Figure 7). This was different from the conformation in compound **15**. Combined with the ROESY correlations of H-7 with H-2ax, H-4ax and H-9ax (δ_H 2.16), the relative configuration of **16** was constructed as shown (Figure 7).

Phyllanthacidoid P (**17**), has a molecular formula $C_{36}H_{51}NO_{20}$, and its NMR data (Tables 6 and 7) were comparable to those of **15**, except that an additional ketal carbon (δ_C 107.1) and methoxyl group (δ_C 50.0), replaced the oxymethine at δ_C 76.9 (C-5) in **15**. The signals at δ_C 107.1 and δ_C 50.0 were assigned to be C-5 and 5−OCH₃, on the basis of the HMBC correlations from H-7, H-3, H-4, and the methoxy protons (δ_H 3.35, OCH₃) to the ketal carbon. The relative configuration of the aglycon was constructed as compound **16**.

The molecular formulas of phyllanthacidoids Q and R (**18** and **19**) were assigned as $C_{35}H_{47}NO_{19}$ and $C_{33}H_{44}O_{19}$, respectively, by HRESIMS. In the ^{13}C NMR spectrum of **18**, a ketone group at δ_C 212.0 replaced the corresponding oxymethine (δ_C 71.4) in **15**, and downfield of C-2 ($\Delta\delta$ 10.0), C-5 ($\Delta\delta$ 8.0) and C-6 ($\Delta\delta$ 7.0) were observed, relative to **15**. The ^1H−^1H COSY data of **18** allowed the connection of the fragment of C(2)H₂/C(3)H/C(4)H₂/C(5)H.

Table 5. ^{13}C and ^{1}H NMR Spectroscopic Data for Compounds 12−14 in CD$_3$OD (δ in ppm)

	12		13		14	
no.	δ_C, mult[a]	δ_H[b]	δ_C, mult[c]	δ_H[b]	δ_C, mult[a]	δ_H[b]
1	65.9, CH	4.14 ddd (8.5, 5.0, 5.0)	66.1, CH	4.16 ddd (9.0, 5.4, 5.4)	65.9, CH	4.12 ddd (9.0, 5.5, 5.5)
2	31.0, CH$_2$	1.84 ddd (14.0, 8.5, 8.5)	30.8, CH$_2$	1.83 ddd (14.4, 9.0, 9.0)	30.0, CH$_2$	1.75 ddd (13.9, 9.0, 9.0)
		2.01 ddd (14.0, 5.0, 5.0)		2.04 m		2.03[d]
3	35.0, CH	2.65 m	34.9, CH	2.68 m	34.3, CH	2.70 m
4	29.9, CH$_2$	1.75 m	30.0, CH$_2$	1.78 ddd (4.1, 10.0, 14.0)	30.0, CH$_2$	1.65 ddd (3.8, 11.5, 14.7)
				2.02 m		1.93 dt (14.7, 4.5)
5	74.5, CH	4.42 dt (8.5, 4.5)	74.6, CH	4.46 dt (8.3, 4.1)	74.6, CH	4.46 dt (8.1, 4.5)
6	47.8, CH	2.36 dt (8.5, 6.5)	47.9, CH	2.37 dt (8.3, 6.5)	48.0, CH	2.34 dt (8.1, 6.1)
7	78.1, CH	3.98 d (6.5)	78.2, CH	4.01 d (6.5)	78.2, CH	3.98 d (6.1)
8	102.7, C		102.6, C		102.5, C	
9	35.9, CH$_2$	2.13 m	36.1, CH$_2$	2.09 dd (2.9, 14.8)	35.7, CH$_2$	2.09[d]
10	72.3, CH	5.26 brs	71.8, CH	5.25 brs	71.6, CH	5.23 brs
11	34.4, CH	2.10 m	34.5, CH	2.09 m	34.4, CH	2.09 m
12	63.3, CH$_2$	3.61 dd (4.0, 11.5)	63.5, CH	3.62 dd (4.3, 11.5)	63.4, CH$_2$	3.61 m
		4.06 dd (11.5, 11.5)		4.08 dd (11.5)		4.05 dd (11.5, 11.5)
13	176.6, C		177.1, C		177.0, C	
14	13.2, CH$_3$	0.89 d (7.0)	13.3, CH$_3$	0.91 d (7.1)	13.1, CH$_3$	0.89 d (7.0)
1′	132.4, C		123.7, C		123.2, C	
2′,6′	130.9, CH	8.11 d (8.0)	133.3, CH	8.01 d (8.9)	133.5, CH	8.03 d (8.9)
3′,5′	129.5, CH	7.49 t (8.0)	116.3, CH	6.88 d (8.9)	116.4, CH	6.88 d (8.9)
4′	134.2, CH	7.62 t (7.5)	163.7, C		163.5, C	
7′	168.2, C		168.5, C		168.2, C	
1″	70.4, CH	4.67 m	70.7, CH	4.71 ddd (4.8, 9.4, 12.2)	70.5, CH	4.74 ddd (4.7, 9.4, 12.0)
2″	82.8, CH	3.54 dd (9.5, 9.5)	83.2, CH	3.60 dd (9.4, 9.4)	86.1, CH	3.44 dd (9.4, 9.4)
3″	76.6, CH	3.28 dd (9.5, 9.5)	76.6, CH	3.32 dd (9.4, 9.4)	76.0, CH	3.38[d]
4″	78.2, CH	3.17 dd (9.5, 9.5)	78.6, CH	3.26 dd (9.4, 9.4)	78.2, CH	3.32[d]
5″	69.6, CH	3.40 m	69.7, CH	3.45 ddd (4.6, 9.1, 12.2)	69.8, CH	3.46 m
6″	35.9, CH$_2$	1.32 q (12.0)	35.9, CH$_2$	1.41 q (12.2)	35.6, CH$_2$	1.45 q (12.0)
		2.04 m		2.10 m		2.10 m
1‴	102.5, CH	4.66 d (8.5)	103.1, CH	4.64 d (8.3)	106.2, CH	4.21 d (8.0)
2‴	58.3, CH	3.51 dd (8.5, 9.3)	58.5, CH	3.53 dd (8.3, 9.6)	75.8, CH	3.15 dd (8.0, 9.0)
3‴	76.8, CH	3.40 dd (9.3, 9.3)	76.9, CH	3.41 dd (9.1, 9.6)	77.9, CH	3.36[d]
4‴	71.7, CH	3.34[d]	71.7, CH	3.39[d]	70.9, CH	3.33[d]
5‴	77.8, CH$_2$	3.04 ddd (1.5, 5.0, 9.0)	77.9, CH$_2$	3.04 ddd (2.7, 4.0, 9.2)	77.8, CH$_2$	2.90 ddd (2.5, 3.5, 9.5)
6‴	62.5, CH$_2$	3.65 dd (5.0, 12.0)	62.5, CH$_2$	3.67 m	62.1, CH$_2$	3.58 dd (2.0, 12.0)
		3.72 dd (1.5, 12.0)				3.63 dd (3.5, 12.0)
1⁗	174.5, C		174.8, C			
2⁗	23.1, CH$_3$	2.00 s	23.2, CH$_3$	2.05 s		

^{a,c}Data were recorded at 100 and 150 MHz, respectively. ^{b}Data were recorded at 600 MHz. ^{d}Signals were overlapped with each other or by solvents.
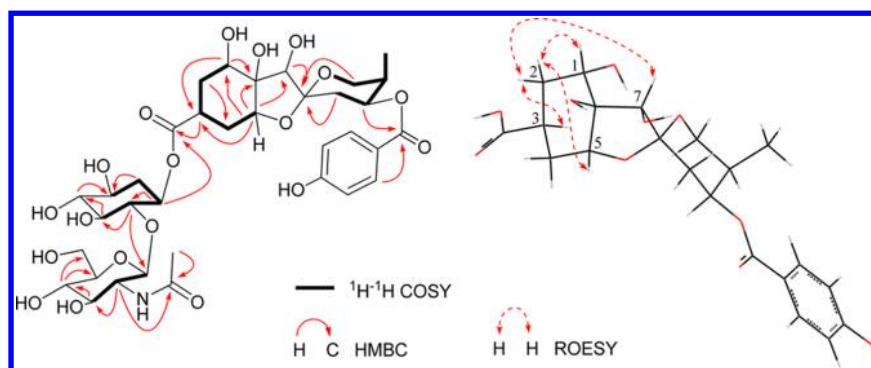
Figure 6. Key HMBC, ^{1}H−^{1}H COSY and ROESY correlations of **15**.

Together with the HMBC correlations from H-2 and H-5 to δ_C 212.0, the ketone group was assigned as C-1. Taking account of other 2D NMR data, the planar structure of **18** was constructed as shown in Figure 8. The axial orientation of H-3 was supported by its large J value (ddd, J = 3.1, 7.8, 11.5 Hz), while the small J value of H-5 (t, J = 3.9 Hz) suggested its equatorial orientation, on the opposite face of H-3. This was confirmed by the ROESY correlations of H-3 with H-4eq (δ_H 2.55), and H-5 with H-4ax. Ring C had the same relative

Table 6. ^{13}C NMR Spectroscopic Data for Compounds 15−19 in CD$_3$OD (δ in ppm)^a

no.	15	16	17	18	19
1	71.4, CH	72.5, CH	72.8, CH	212.0, C	212.0, C
2	32.3, CH$_2$	31.8, CH$_2$	31.6, CH$_2$	42.3, CH$_2$	42.1, CH$_2$
3	33.3, CH	37.4 CH	36.2 CH	36.9, CH	36.8, CH
4	28.4, CH$_2$	37.4, CH$_2$	31.8, CH$_2$	32.0, CH$_2$	31.9, CH$_2$
5	76.9, CH	105.3, C	107.1, C	84.9, CH	84.9, CH
6	78.6, C	80.9, C	79.9, C	85.6, C	85.5, C
7	90.2, CH	78.8, CH	78.9, CH	87.7, CH	87.7, CH
8	108.6, C	108.2, C	110.2, C	109.9, C	110.1, C
9	30.4, CH$_2$	33.1, CH$_2$	32.8, CH$_2$	30.8, CH$_2$	30.8, CH$_2$
10	71.7, CH	71.6, CH	71.5, CH	71.8, CH	71.7, CH
11	33.8, CH	33.9, CH	33.9, CH	33.9, CH	33.9, CH
12	66.1, CH$_2$	67.0, CH$_2$	67.7, CH$_2$	65.8, CH$_2$	65.8, CH$_2$
13	176.9, C	175.6, C	175.6, C	175.6, C	175.6, C
14	10.7, CH$_3$	10.7, CH$_3$	10.8, CH$_3$	10.9, CH$_3$	10.9, CH$_3$
1′	122.4, CH	122.6, CH	122.9, CH	122.5, CH	122.5, CH
2′,6′	132.9, CH	132.8, CH	132.9, CH	133.0, CH	133.0, CH
3′,5′	116.4, CH	116.3, CH	116.4, CH	116.4, CH	116.3, CH
4′	164.0, C	163.8, C	163.9, C	164.0, C	164.0, C
7′	167.6, C	167.4, C	167.5, C	167.6, C	167.6, C
1″	70.3, CH	70.8, CH	71.1, CH	71.0, CH	71.0, CH
2″	82.8 CH	85.7, CH	82.1, CH	81.5, CH	83.5, CH
3″	76.5, CH	76.0, CH	76.8, CH	76.9, CH	76.4, CH
4″	78.8, CH	78.3, CH	78.9, CH	78.8, CH	78.3, CH
5″	69.7, CH	69.9, CH	69.8, CH	69.7, CH	70.0, CH
6″	35.9, CH$_2$	35.4, CH$_3$	36.0, CH$_3$	35.9, CH$_2$	35.9, CH$_2$
1‴	102.7, CH	105.9, CH	102.7, CH	102.3, CH	104.5, CH
2‴	58.4, CH	76.0, CH	58.5, CH	58.5, CH	76.0, CH
3‴	76.8, CH	78.3, CH	77.1, CH	76.9, CH	78.3, CH
4‴	72.7, CH	71.2, CH	72.2, CH	72.7, CH	71.9, CH
5‴	78.1, CH	78.7, CH	78.2, CH	78.4, CH$_2$	78.4, CH$_2$
6‴	63.3, CH$_2$	62.6, CH$_2$	62.9, CH$_2$	63.4, CH$_2$	63.0, CH$_2$
1⁗	174.6, C		174.5, C	174.6, C	
2⁗	23.1, CH$_3$		23.1, CH$_3$	23.2, CH$_3$	
5−OCHH$_3$		50.0, CH$_3$			

^{a}Data were recorded at 150 MHz.

Figure 7. Key ROESY correlations of **16**.

configuration as those of **15−17**. The ROESY correlation of H-7 with H-9ax allowed the assignment of H-7 as α-orientation, and strong ROESY correlation of H-5 with H-4ax indicated the β-orientation of H-5. Additionally, the ROESY correlations of H-3 with H-12 indicated that both H-3 and C-12 had the α-orientation. On the basis of the above evidence, the relative configurations of all the stereogenic centers of **18** except C-6 were established (Figure 8). Phyllanthacidoid R (**19**) had the same aglycon part as that of **18**, and the saccharide moiety was determined to be *scyllo* quercitol-2-O-β-glucose by comparison of NMR data (Tables 6 and 7).

Phyllanthacidoids S-T (**20−21**) had molecular formulas $C_{35}H_{49}NO_{20}$ and $C_{33}H_{46}O_{20}$, respectively, as established from HRESIMS. The ^{13}C NMR data of **20** (Table 8) were similar to those of **7**, except for chemical shifts changes of C-1 ($\Delta\delta$ 3.7), C-4 ($\Delta\delta$ −3.8), C-7 ($\Delta\delta$ 3.7), C-8 ($\Delta\delta$ 4.8), C-11 ($\Delta\delta$ 5.9), C-12 ($\Delta\delta$ 3.4). The fragments of CH(1)/CH$_2$(2)/CH(3)/CH(4), CH$_2$(9)/CH(10)/CH(11)/CH$_2$(12) and CH(11)/CH$_3$(14) were constructed by ^{1}H−^{1}H COSY spectrum (Figure 9). The HMBC correlations (Figure 9) from H-1 to C-5/C-6, H-9 to C-7/C-8, H-7 to C-5, H-4 to C-5 and C-3, H-10 to C-8 revealed a 6/5-fused rings in **20**, similar to that of **7**. However, there was an HMBC correlation from H-1 to C-8, but no HMBC correlation from H-12 to C-8 in **7**, suggesting that the C-8/C-12 ether bond in 5/6-spiro ring system in **7** was opened, and an oxygen bridge between C-1 and C-8 was formed to construct an additional tetrahydrofuran ring in **20**. Correspondingly, the C ring was opened in **20** to form an aliphatic chain fragment from C-9 to C-12. The signals of H-12 and the benzoyl protons (δ_H 7.90, 6.84) were correlated to the benzoyl carboxyl carbon C-7′ in HMBC spectrum, which allowed the connection of the *p*-hydroxybenzoate to C-12. Thus, the planar structure of **20** was constructed, which possessed an unusual fused tetrahydrofuran skeleton formed by a 5, 8-diketal system.

The small double doublet couplings of H-1 (1.3, 3.3 Hz) indicated its equatorial orientation, and the large coupling of H-3 (13.0 Hz) showed its axial orientation, on the opposite face of H-1. The α-orientation of H-7 was confirmed by the NOE effects between H-1 and H-7, while the large coupling constants of H-9a (δ_H 1.94, 1H, dd, J = 10.1, 14.8 Hz) suggested its anti orientation to H-10. Together with the ROESY correlation between H-9a and H-7, the relative configurations of **20** could be constructed, except for the fragment of C10−C11 (Figure 9).

The coupling constant of $J_{H-10,H-11}$ = 5.7 Hz suggested that the conformation of C-10 and C-11 was a mixture of gauche and anti rotamers, whose relative configuration was not able to be constructed on the basis of the ROESY correlations and ^{1}H−^{1}H coupling constants. The relative configuration of C-10 and C-11 was determined using Murata's method,[15] since the fragment C10−C11 had a methyl and an oxygen substituted 1,2-methine system. All the $^{2,3}J_{C,H}$ were accurately measured from a HETLOC 2D NMR spectrum (Figure S149−153 in Supporting Information). The medium value (5.7 Hz) of $^3J_{H-11,H-10}$ indicated that the 1,2 methine system of C10−C11 was an alternating pair of gauche and anti rotamers, which ruled out A1/A2 and B1/B2. A small heteronuclear $^3J_{H-10, C-14}$ value (2.8 Hz) showed a gauche configuration of H-10 and 14-methyl, and this ruled out A1/A3 and B1/B3 pairs with medium $^3J_{H-10, C-14}$. Additionally, a medium $^2J_{H-11, C-10}$ value of −2.5 Hz indicated the coexistence of gauche and anti configuration of 10-OH and H-11, which ruled out A2/A3, and left B2/B3 as the correct rotamer pair. This result was confirmed by the ROESY correlations of H-10 with H-11 and H-14 (in B2). Meanwhile, ROESY correlation between H-9 and H-14 (in B3) was also observed. Thus, with the results obtained using Murata's rules, the relative configuration of C10−C11 in **20** was established as 10S*,11R* (Figure 10). The aglycon of **21** was the same as that of **20**, on comparison with the ^{1}H and ^{13}C NMR (Table 8). However, the saccharide moiety of **21** was determined to be *scyllo* quercitol 2-O-β-glucopyranose.

Tautomerism of 5-Hemiketal Compounds (7−9, and 16). Compounds **7−9** and **16** are 5-hemiketals, whose B rings are able to be opened and recycled to form the 5R isomers. In the case of compound **7**, if it was stored in solution for several days, two peaks (rt 11.5 min for **7** and 14.7 min for 5R-**7**) were detected by

Table 7. ^{1}H NMR Spectroscopic Data for Compounds 15–19 in CD$_3$OD (δ in ppm)^a

no.	15	16	17	18	19
1	4.04 t (3.2)	4.15 dd (5.1, 11.4)	4.03 dd (3.8, 8.4)		
2	1.88^b	1.67 ddd (4.5, 11.4, 14.0)	1.96 ddd (5.7, 8.4, 13.7)	2.64 d (9.4)	2.61 d (9.8)
	2.03^b	2.29 brd (14.0)	2.11^b		
3	3.10 tt (3.5, 12.5)	3.02 m	2.87 tt (5.7, 8.1)	3.39 ddd (3.1, 7.8 11.5)	3.42 m
4	1.89^b	2.13^b	2.12^b	1.98 ddd (3.9, 11.5, 14.4)	1.96 ddd (3.6, 11.4, 14.4)
	2.32 brd (14.6)	2.44 brd (14.7)	2.21^b	2.55 brd (14.4)	2.52 brd (14.4)
5	4.08 t (3.1)			4.33 t (3.9)	4.30 t (3.6)
7	4.16 s	4.31 s	4.13 s	3.94 s	3.94 s
9	2.05^b	1.96 dd (4.6, 12.7)	2.02 dd (4.4, 13.2)	2.00^b	2.00 dd (12.1, 12.6)
		2.16^b	2.13^b	2.15^b	2.16 m
10	5.50 dt (11.6, 5.1)	5.50 dt (11.8, 4.3)	5.55 dt (11.7, 4.4)	5.55 dt (11.9, 5.1)	5.53 dt (12.1, 5.0)
11	2.18 m	2.23 m	2.21^b	2.26 m	2.24 m
12	3.49 dd (1.2, 11.7)	3.56 brd (12.1)	3.62 brd (12.1)	3.55 dd (1.7, 11.7)	3.58 dd (1.6, 11.6)
	4.15 dd (2.1, 11.7)	4.19 brd (12.1)	4.21 brd (12.1)	4.17 dd (2.5, 11.7)	4.15 dd (2.5, 11.6)
14	1.17 d (7.1)	1.16 d (7.1)	1.23 d (7.1)	1.17 d (7.0)	1.17 d (7.1)
2′,6′	7.91 d (8.9)	7.88 d (8.8)	7.88 d (8.6)	7.91 d (8.8)	7.90 d (8.8)
3′,5′	6.85 d (8.9)	6.84 d (8.8)	6.84 d (8.6)	6.86 d (8.8)	6.85 d (8.8)
1″	4.80 ddd (4.8, 9.5, 12.0)	4.79 ddd (4.8, 9.8, 12.0)	4.71 ddd (4.8, 9.8, 12.0)	4.78 ddd (4.9, 9.7, 12.1)	4.83 ddd (4.9, 9.8, 12.4)
2″	3.76 dd (9.5, 9.5)	3.69 dd (9.5, 9.5)	3.79 dd (9.5, 9.5)	3.87 dd (9.5, 9.5)	3.83 dd (9.6, 9.6)
3″	3.35^b	3.43 dd (9.5, 9.5)	3.32^b	3.33^b	3.44 dd (9.6, 9.6)
4″	3.24 dd (9.5, 9.5)	3.27 dd (9.5, 9.5)	3.20 dd (8.9, 8.9)	3.22 dd (9.3, 9.3)	3.26 dd (9.6, 9.6)
5″	3.47 m	3.47 m	3.45 m	3.46 m	3.49 ddd (4.5, 9.4, 12.4)
6″	1.52 q (12.0)	1.52 q (12.0)	1.49 q (12.0)	1.54 q (12.1)	1.56 q (12.4)
	2.14 dt (4.6, 12.0)	2.22^b	2.18^b	2.14 m	2.16^b
1‴	4.80 d (8.3)	4.58 d (8.1)	4.86 d (8.5)	4.90 d (8.4)	4.71 d (8.0)
2‴	3.57 dd (8.3, 10.1)	3.23 dd (8.1, 9.2)	3.58 dd (8.5, 10.3)	3.60 dd (8.4, 10.1)	3.22 dd (8.0, 9.0)
3‴	3.46^b	3.38^b	3.41 dd (8.7, 10.3)	3.46 dd (8.4, 10.1)	3.40 dd (9.0, 9.0)
4‴	3.32^b	3.30 dd (8.6, 8.6)	3.35^b	3.35^b	3.35 dd (9.0, 9.0)
5‴	3.30 ddd (2.2, 6.6, 9.3)	3.28 m	3.25 ddd (2.4, 5.8, 9.6)	3.31 m	3.34^b
6‴	3.83 dd (6.6, 11.8)	3.71 dd (6.4, 11.8)	3.79^b	3.82 dd (6.0, 12.0)	3.80 dd (5.7, 12.4)
	3.94 dd (2.2, 11.8)	3.87 dd (1.9, 11.8)	3.90 dd (2.2, 11.8)	3.99 dd (2.3, 12.0)	3.97 dd (2.1, 12..4)
2⁗	2.02 s		2.00	2.02 s	
5−OCHH$_3$			3.35		

^{a}Data were recorded at 600 MHz. ^{b}Signals were overlapped with each other or by solvents.
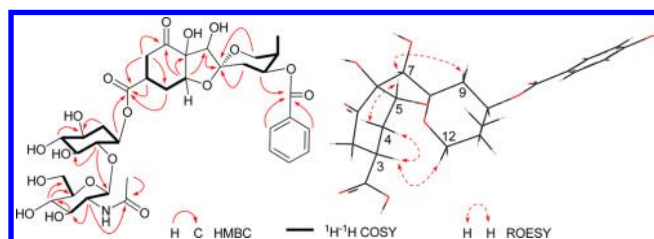
Figure 8. Key HMBC, ^{1}H−^{1}H COSY, and ROESY correlations of **18**.

HPLC analysis (Figure 11-B). The preparative HPLC (p-HPLC) was carried out to separate **7** and 5*R*-**7**, and HPLC analysis with the same conditions was repeated to get the results as shown in Figure 11-C and 11-A. It was noted that both 5*S* (Figure 11-C) and 5*R* (Figure 11-A) isomers existed as a mixture of both tautomers, and the 5*S* isomer was the main constituent (4.1/1 in 5*S* isomer, and 1.8/1 in 5*R* isomer). This was confirmed by the similar ^{1}H NMR spectra of 11-A and 11-C (Figure S50 in Supporting Information). The ratio of 5*S*/5*R* also suggested that the 5*S* isomer was more stable than the 5*R* isomer. This means that although the 5*R* isomer was easily separated from the 5*S* isomer due to the large Δrt, it was inclined to tautomerize to the 5*S* isomer. This is why we did not obtain compounds **7**−**9** and **16** with the 5*R* configuration, and it also can explain the minor impurity of these four compounds in their NMR spectra. During

the process of extraction, 5-ketal compound **11** was likely to be produced from **7** with the participation of methanol, especially at high temperature under reflux conditions. Thus, the 5-ketal compounds **10**, **11** and **17** may be artifacts produced from the corresponding 5-hemiketal precursors.

Absolute Configurations. The Abs of the isolated compounds were determined using quantum chemical methods. The conformation search was carried out using molecular mechanics MMFF. The resulted conformers (<25 kJ mol^{-1}) were optimized using DFT at the B3LYP-SCRF/6-311G(d, p) level. The optimized low energy conformers with population <1% were considered for ECD calculation. The TD-DFT/ B3LYP-SCRF/6-311G(d, p) method was applied to calculate the ECD spectra of each conformer by introducing the Gaussian Function, with a band shape 0.5 eV. The final ECD spectra were obtained by averaging all the simulated ECD spectra of the calculated conformers according to Boltzmann distribution.

All the Abs of the isolated compounds except for **20** and **21** were determined by comparing the TDDFT calculated ECD curves with those of the experimental ones. This is possible because the benzoyl moiety adjacent to the C*-10 stereo center, is located on a tetrahydropyran ring, with a rigid environment. This structural feature makes it easy to find out the stable conformer during the ECD calculation, and produce reliable results. The Cotton effects at 240 and 260 nm produced by the

Table 8. ^{13}C NMR and ^{1}H NMR Spectroscopic Data for Compounds 20−21 in CD$_3$OD (δ in ppm)^a

	20		21	
no.	δ_C, mult	δ_H	δ_C, mult	δ_H
1	75.7, CH	4.13 dd (1.3, 3.3)	75.7, CH	4.03 brs
2	28.2, CH$_2$	1.64 ddd (1.3, 13.0, 14.4) 2.15^b	28.1, CH$_2$	1.64 ddd (1.4, 13.0, 14.6) 2.13^b
3	35.7, CH	2.91 ddd (3.9, 13.0, 13.0)	35.6, CH	2.93 tt (3.6, 13.0)
4	32.5, CH$_2$	1.80 d (13.0)	32.8, CH$_2$	1.80 dd (13.0, 13.5)
				2.05 dd (3.6, 13.5)
5	103.1, C		103.1, C	
6	76.8, C		77.0, C	
7	79.8, CH	3.89 s	79.8, CH	3.89 s
8	107.6, C		107.6, C	
9	36.4, CH$_2$	1.94 dd (10.1, 14.8) 2.12^b	36.4, CH$_2$	1.92 dd (10.1, 14.8) 2.08^b
10	70.0, CH	3.99 ddd (1.8, 5.7, 10.1)	70.0, CH	4.01 ddd (1.7, 5.9, 10.1)
11	40.1, CH	2.09^b	40.0, CH	2.10^b
12	67.3, CH$_2$	4.24 dd (6.5, 11.4)	67.4, CH$_2$	4.25 dd (6.5, 11.0)
		4.34 dd (5.8, 11.4)		4.31 dd (5.8, 11.0)
13	175.8, C		176.1, C	
14	14.1, CH$_3$	1.07 d (7.0)	14.0, CH$_3$	1.07 d (7.0)
1′	122.5, CH		122.6, CH	
2′,6′	133.0, CH	7.90 d (8.9)	133.0, CH	7.90 d (8.8)
3′,5′	116.4	6.84 d (8.9)	116.4, CH	6.84 d (8.8)
4′	163.7, C		163.7, C	
7′	168.5, C		168.4, C	
1″	70.8, CH	4.75 ddd (4.7, 9.5, 12.2)	70.7, CH	4.81 m
2″	82.7, CH	3.76 dd (9.5, 9.5)	85.0, CH	3.72 dd (9.4, 9.4)
3″	76.7, CH	3.31^b	76.2, CH	3.41 dd (9.4, 9.4)
4″	78.9, CH	3.20 dd (9.3, 9.3)	78.2, CH	3.25 dd (9.4, 9.4)
5″	69.7, CH	3.45^b	69.9, CH	3.45^b
6″	35.9, CH$_2$	1.47 q (12.2) 2.06^b	35.9, CH$_2$	1.51 q (12.1) 2.11^b
1‴	102.8, CH	4.79 d (8.5)	105.7, CH	4.55 d (8.0)
2‴	58.5, CH	3.54 dd (8.5, 10.2)	76.1, CH	3.18 dd (8.0, 8.8)
3‴	77.0, CH	3.43 dd (8.8, 10.2)	78.3, CH	3.33^b
4‴	72.4, CH	3.30^b	71.6, CH	3.30^b
5‴	78.2, CH$_2$	3.25 ddd (2.3, 6.3, 9.7)	78.3, CH$_2$	3.22 ddd (2.5, 5.0, 9.6)
6‴	63.2, CH$_2$	3.77 dd (6.3, 11.9)	62.7, CH$_2$	3.74 dd (5.0, 11.5)
		3.90 dd (2.3, 11.9)		3.88 dd (2.5, 11.5)
1⁗	174.7	2.00 s		
2⁗	23.2			

^{a}Data were recorded at 600 MHz for ^{1}H, and 150 MHz for ^{13}C NMR. ^{b}Signals were overlapped with each other or by solvents.
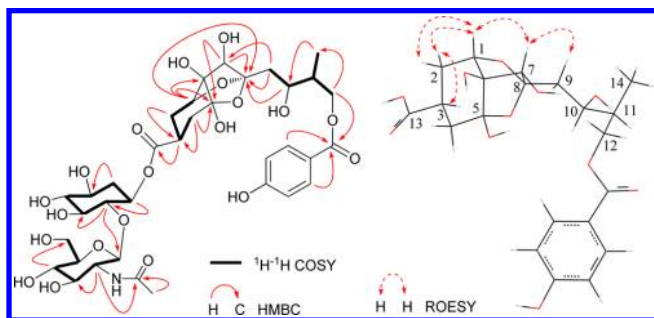
Figure 9. Key HMBC, ^{1}H−^{1}H COSY, and ROESY correlations of 20.

p-hydroxyl benzoyl moiety, and 230 and 250 nm produced by the benzoyl moiety are diagnostic for the absolute configurations of
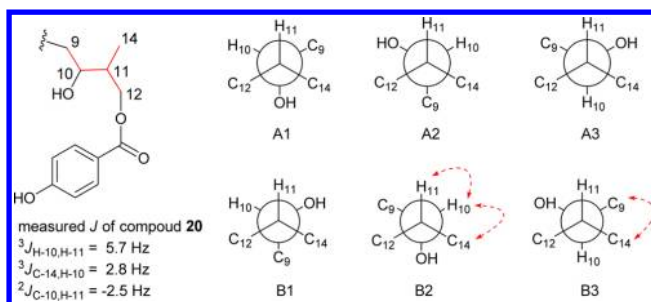
Figure 10. Newman projection of all possible staggered rotamers of *threo* and *erythro* configurations viewed down bonds C11−C10. The $^3J_{H,H}$ and $^{2,3}J_{C,H}$ values allowed the assignment of rotamers of B2/B3, and the ROESY correlations were drawn in dashed line double-headed arrows.
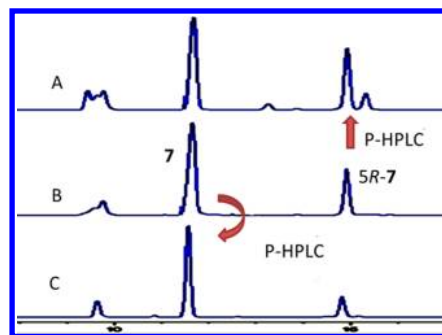
Figure 11. HPLC chromatograms of 7 and 5*R*-7. (A) p-HPLC prepared 5*R*-7; (B) stored sample of 7; (C) p-HPLC prepared 7.

ring C. For compounds **1−14**, the experimental ECD spectra displayed negative Cotton effects at 230 or 240 nm, and positive Cotton effects at 250 or 260 nm, which agreed well with the calculated ECD curves of 8*S*, 10*S*, 11*R* isomers (Figure 12-1, 2). Since the relative configurations of the tetrahydropyran ring C in **1−14** can be constructed on the basis of the coupling constants analysis, it can be concluded that there are two possible enantiomers of ring C, i.e., 8*S*,10*S*,11*R* isomer with the Cotton effects as shown in Figure 12-1 and 2, and 8*R*,10*R*,11*S* isomer with the mirror image Cotton effects of 8*S*,10*S*,11*R* isomer. Thus, the Abs of **1−14** can also be established by comparing the calculated and experimental ECD curves, even though there are no NOE effects from ring A and B to ring C to construct the relative configuration of C-8. This situation occurred more or less for compounds **2−14** because of the proton signals overlapping of H-9 with H-2 and H-11.

The ECD spectra of **15−19** were different from those of **1−14**, of which the positive effects at 260 nm had opposite signs, and displayed a broad negative Cotton effect at 240−260 nm (Figure 12-3 and 12-4). This ECD characteristic was consistent with the calculated ECD curves of 8*R*,10*S*,11*R* isomers (Figure 12-3 and 12-4a), rather than that of 8*S*,10*R*,11*S* isomer with the positive Cotton effects at 240−260 nm (Figure 12-4b). The above results indicated that the sign of the Cotton effect at 260 nm represented the Ab of C-8, 8*S* (+) and 8*R* (−), while the sign of the strong Cotton effect at 240 nm corresponded to the Ab of C-10, 10*S* (−) and 10*R* (+). As in the case of **1−14**, the Abs of compounds **15−19** could be established by comparing the calculated and experimental ECD curves, which were independent of the relative configuration from rings A and B to C. Thus, the four possible stereoisomers of ring C displayed distinguishable Cotton effects, which can become a method to determine the Abs of this type of compounds.
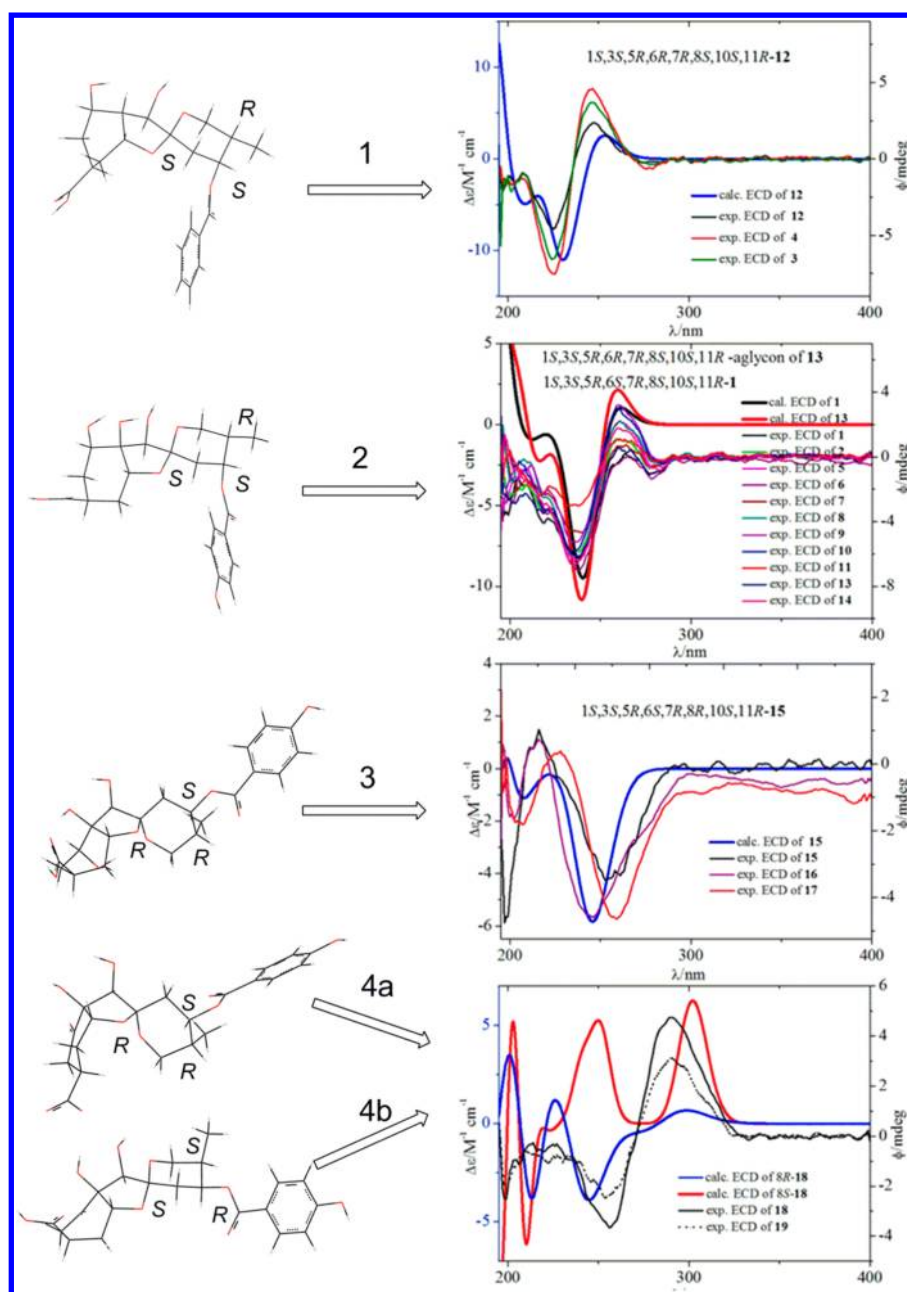
Figure 12. Calculated and experimental ECD curves of compounds **1**−**19**.

It is difficult to determine the relative configuration of C-6 for compounds **18** and **19**, because of the existence of a carbonyl at C-1. However, the carbonyl in the cyclohexanone moiety generated a strong Cotton effect at 300 nm (Figure 12-4), which made it easy to determine the Ab of C-6 by TDDFT calculated ECD. With the above results, it can be concluded that, except for the ketal carbon C-8, the Abs of the norbisabolane type sesquiterpenoids tends to remain the same. Finally, on the basis of the relative configurations established by means of coupling constants analysis and ROESY correlations, the Abs of **1**−**19** were established unambiguously.

Determination of Abs of **20** and **21** was challenging because of the location of chromophore on an aliphatic chain, and the ECD method was limited. Since the Abs of C1−C8 in **1**−**19** remained the same, it could be proposed that C1−C8 also had the same Abs in **20** and **21**. On this basis, the Ab of the aliphatic chain was determined by comparing DFT/MPW1PW91 6-31G(d, p)[16]

calculated J values with experimental results, considering that the large substituent (C-8) at C-9 may affect the conformation of the aliphatic chain. Of the calculated four isomers of C-10 and C-11, only the 10S,11R isomer agreed well with the experimental results (Table 9), with the mean absolute error (MAE) 0.7 Hz. This result was consistent with the conclusion obtained for compounds **1**−**19**. However, the low energy conformers of 10S,11R isomer mainly composed of B1 (64%) and B3 (31%) conformers, rather than the conformers B2/B3 determined by Murata's method (Figure 10). Despite using Murata's method can lead to correct assignment of *erythro* relative configuration of **20**, it should be careful when applying this method to the 1,2-methine system with large substituents.

Anti-HBV Activities of Isolated Compounds. The virus strains of H3N2, EV71, HSV-1, and CVB3 were unaffected by the main constituents **2** and **3**, which agreed with the preliminary screening results for the methanolic extract and sesquiterpenoid

Table 9. DFT Calculated and Experimental NMR J Values of Aliphatic Chain (Hz)

items	$J_{C14,H10}$	$J_{C10,H11}$	$J_{H9a,H10}$	$J_{H9b,H10}$	$J_{H10,H11}$	$J_{H11,H12a}$	$J_{H11,H12b}$	MAE
exp.	2.8	−2.5	10.1	1.8	5.7	6.5	5.8	
calc. 10S,11R	3.3	−2.4	8.6	1.8	6.0	8.2	5.2	0.7
calc. 10R,11S	1.7	−3.4	9.8	1.0	9.1	2.9	1.7	2.1
calc. 10R,11R	4.8	1.9	9.6	1.5	2.3	10.2	4.4	2.2
calc. 10S,11S	4.8	1.8	9.5	1.3	2.4	10.3	4.6	2.2

enriched fraction. Nine of the isolates (**1**−**4**, **7**−**9**, **10** and **14**) were further tested for their in vitro anti-HBV activities. As shown in Table 10, all of them exhibited inhibitory activity, with

Table 10. Anti-HBV Activity (IC$_{50}$ μM for Pure Compounds, and μg mL^{-1} for Extracts and Fraction)^a

compounds	HBV		
	HBsAg IC$_{50}$/SI^c	HBeAg IC$_{50}$/SI	CC$_{50}$^{b}
1	28.8/3.6	NA^d	104.0
2	NA	12.5/1.5	19.2
3	NA	6.6/3.8	24.8
4	NA	0.8/1.9	1.5
7	24.3/2.1	24.0/2.1	51.4
8	15.1/4.0	22.2/2.7	60.0
9	25.9/10.8	35.8/7.8	279.7
10	NA	25.9/6.4	165.5
14	NA	2.3/1.0	2.3
methanol extracts	38.6/4.6	39.0/4.5	177.2
sesquiterpenoids fraction	31.0/2.7	28.7/2.9	82.5

^{a}Lamivudine was tested as the positive control of anti-HBV. The inhibition ratio against HBsAg and HBeAg were 44.66 ± 2.09 and 25.96 ± 9.59 (100 μM); 31.56 ± 9.21 and 18.67 ± 3.16 (10 μM). ^{b}Compound concentration reducing the viability of HepG2.2.2.15 cells culture by 50%. ^{c}SI = CC$_{50}$/IC$_{50}$. ^{d}Not active below the concentration of CC$_{50}$.

compounds **4** and **14** being the most potent. It is noted that this type of highly oxygenated norbisabolane sesquiterpenoids are specifically effective against HBV. Compounds **2**−**4** can selectively affect the secretion of HBeAg, with **4** being more potent with an IC$_{50}$ of 0.8 μM, but their aglycon **1** can specifically affect the secretion of HBsAg with IC$_{50}$ of 28.8 μM. Phyllanthacidoids F−H (**7**−**9**) featured a 5-hemiketal group, and all of them showed inhibition toward both HBsAg and HBeAg. When the hydroxyl group at the 5-hemiketal carbon was methylated; e.g., **10**, the inhibitory activity against HBsAg was lost. The cytotoxicities (CC$_{50}$) on HepG2.2.2.15 cells of the tested compounds were also evaluated and shown in Table 10. Compound **14** with a 5,6-dimethine structure had equal CC$_{50}$ and IC$_{50}$ values. Compound **1** as well as the glycosides with a 5-ketal group (**7**−**10**) displayed relatively lower cytotoxicities.

Except for interferon, all FDA approved antiviral drugs are nucleoside or nucleoside based polymerase inhibitors,[17] and the tolerance of these drugs stimulated researchers to explore new anti-HBV agents with novel mechanisms. It is believed that the high levels of HBsAg bearing subviral particles in the serum of chronically infected individuals play a role in suppressing the HBV immune response, and current therapeutics are not directed at reducing this antigenemia.[18] The anti-HBV lead compound PBHBV-2−15 was discovered based on the target of HBsAg secretion.[19] Ellagic acid, a phenolic compound isolated from *Phyllanthus urinaria*, displayed unique anti-HBV mechanism, which can specifically inhibit HBeAg secretion, rather than

HBsAg.[20] Although the anti-HBV mechanism of the isolated compounds is still unknown, their effects to HBsAg and HBeAg secretion are potential, and the structure dependent selectivity to HBsAg and HBeAg are unique. The reported sesquiterpenoid glycosides with unusual structures add a new class of anti-HBV compounds, which are promising for development as anti-genemia agents. Our further studies will focus on the anti-HBV mechanism, structure−activity relationships and the structure modifications in order to minimize the cytoxicities of this type of compounds.

■ EXPERIMENTAL SECTION

General Experimental Methods. 1D and 2D NMR spectra were run on 400, 500, 600, and 800 MHz NMR spectrometers for ^{1}H, and 100, 125, and 150 MHz for ^{13}C, respectively. Coupling constants are expressed in Hertz and chemical shifts are given on a ppm scale with solvents as internal standard. ESI-MS and HRESIMS were measured at TOF-MS spectrometer. The preparative HPLC was performed with a HPLC equipped with a DAD detector. Column chromatography was performed with Sephadex LH-20, Diaion HP20SS, CHROMATOREX ODS, Amberchrom CG161M, Rp-8 gel (40−60 μm), Toyopearl HW-40C, Silica gel (200−300 mesh and a 250 × 9.4 mm, i.d., 5 μm C$_{18}$ column. TLC was carried out on precoated silica gel GF254 plates, which were visualized by ultraviolet and spraying with 10% sulfuric ethanol solution. The quantum chemical calculations were carried out at HPC Center, Kunming Institute of Botany, CAS, China.

Plant Material. The whole plant of *P. acidus* was collected in Hongdong District, Chiangmai, Thailand, in May 2012, and identified by Prof. C. R. Yang (Kunming Institute of Botany, Chinese Academy of Sciences). A voucher specimen (KIB-Z-1205006) has been deposited in the State Key Laboratory of Phytochemistry and Plant Resource in West China of Kunming Institute of Botany, Chinese Academy of Sciences.

Extraction and Isolation. The air-dried roots and stems of *P. acidus* (10 kg) were extracted with refluxing methanol solution three times to give 469 g extract. The extract was suspended in 5.5 L of H$_2$O and partitioned with *n*-BuOH. The organic layer was concentrated in vacuo and subjected to passage over a Diaion HP20SS column, eluting with CH$_3$OH/H$_2$O (0−100%), to afford five major fractions. Fraction 2 (70 g) was chromatographed on Sephadex LH20 (CH$_3$OH/H$_2$O 0−100%) to afford five fractions. The first two fractions (40.3 g) were combined and chromatographed on a silica gel column (CHCl$_3$/CH$_3$OH/H$_2$O, 9:1:0−7:3:0.5) to give seven subfractions (Fr.A−Fr.G). Fr.A was subjected to RP-8 (CH$_3$OH/H$_2$O 30−80%) to afford 8 fractions (Fr.A1-Fr.A8), and Fr.A7 was separated on Toyopearl HW 40C (CH$_3$OH 0−30%) to give 5 fractions (Fr.A7.1−Fr.A7.5). Fr.A7.2 was separated by p-HPLC (CH$_3$CN/H$_2$O 15−30%) to afford **20** (2 mg), **17** (2 mg), and **7** (185 mg). Fr.A4 (300 mg) was passaged over a Toyopearl HW 40C (CH$_3$OH/H$_2$O 0−30%) column to give FrA4.1−4.2. Fr.A4.1 was separated by Amberchrom CG161 M (CH$_3$OH/H$_2$O 40−90%), and p-HPLC (CH$_3$CN/H$_2$O 15−30%) to afford **9** (36 mg). Fr.A5 (600 mg) was subjected to Toyopearl HW 40C (CH$_3$OH/ H$_2$O 0−30%) column to give Fr.A5.1−Fr.A5.2. Fr.A5.1 was chromatographed by Amberchrom CG161 M (CH$_3$OH/H$_2$O 40−90%) to afford Fr.A5.2.1−Fr.A5.2.2, and Fr.A5.2.1 was separated by p-HPLC (CH$_3$CN/ H$_2$O 15−30%) to yield **16** (2 mg). Fr.B (13.2 g) was subjected to CHROMATOREX ODS (CH$_3$OH/H$_2$O 30−80%) to give Fr.B1−Fr.B4, and Fr.B3 was purified on a silica gel column (CHCl$_3$/CH$_3$OH/H$_2$O, 8:3:0.2) to give **2** (10.3 g). Fr.B2 was passaged over Toyopearl HW 40C (CH$_3$OH/H$_2$O 0−30%) to give Fr.B2.1−Fr.B2.2, and Fr.B2.1 was subjected to Amberchrom CG161 M (CH$_3$OH/H$_2$O 40 −90%) to afford

Fr.2.1.1–Fr.2.1.4. Fr.B2.1.2 was separated by p-HPLC (CH_3CN/H_2O 15–30%) to produce **21** (2 mg), and **8** (52 mg). Fr.C passaged over RP-8 (CH_3OH/H_2O 30–80%) to give Fr.C1–Fr.C7, and Fr.C6 (1 g) was subjected to Amberchrom CG161 M (CH_3OH/H_2O 40–90%) to afford Fr.C6.1–6.2. FrC6.2 (150 mg) was purified by p-HPLC (CH_3CN/H_2O 15–30%) to give **18** (17 mg), **15** (2 mg), **11** (10 mg), **5** (9 mg), and **13** (8 mg). Fr.C7 (1.2 g) was subjected to Amberchrom CG161 M (CH_3OH/H_2O 40–90%) to give **3** (1.0 g). Fr.D was chromatographed by RP-8 (CH_3OH/H_2O 30–80%) to afford Fr.D1–Fr.D5, and Fr.D5 (570 mg) was subjected to Amberchrom CG161 M (CH_3OH/H_2O 40–90%) to give Fr.D5.1–Fr.D5.4. Fr.D5.2 (46 mg) was separated by p-HPLC (CH_3CN/H_2O 15–30%) to yield **10** (6 mg). Fr.D5.3 was purified by p-HPLC (CH_3CN/H_2O 15–30%) to give **19** (2 mg), **4** (319 mg), **12** (8 mg), and **14** (17 mg). Fr.E was chromatographed by RP-8 (CH_3OH/H_2O 30–80%) to afford Fr.E1–Fr.E8. Fr.E5 (650 mg) was passaged over Toyopearl HW 40C (CH_3OH/H_2O 0–30%) column to give Fr.E5.1–Fr.E5.3, and Fr.E5.2 (34 mg) was separated by p-HPLC (CH_3CN/H_2O 15–30%) to afford **6** (14 mg). Fr.F was chromatographed by RP-8 (CH_3OH/H_2O 30–80%) to afford Fr.F1–Fr.F6. Fr.F6 (397 mg) was purified by Toyopearl HW 40C (CH_3OH/H_2O 0–30%) column and Amberchrom CG161 M (CH_3OH/H_2O 40–90%) to give **1** (240 mg).

ECD and OR Calculation. The aglycons of the compounds were used as the chemical model to carry out ECD calculation. The conformation analysis was carried out using molecular mechanics MMFF in Sparton'06 (Wave function Inc. Irvine, CA). The resulting conformers (<25 kJ mol^{-1}) were optimized using DFT at the B3LYP-SCRF/6-311G(d, p) level using the integral equation formalism variant of the polarizable continuum model (IEF-PCM). All the calculations were run with Gaussian '09.[21] The free energies and vibrational frequencies were calculated at the same level to confirm their stability, and no imaginary frequencies were found. The optimized low energy conformers with population <1% were considered for ECD calculation. The TD-DFT/B3LYP-SCRF/6-311G(d, p) method was applied to calculate the excited energies, oscillator strength and rotational strength. The excited energies and rotational strength were used to simulate ECD spectra of each conformer by introducing the Gaussian Function. The final ECD spectra and OR of each compound were obtained by averaging all the simulated ECD spectra and ORs of all conformers according to Boltzmann distribution. The ORs were calculated using TDDFT/GIAO with basis set B3LYP/6-311++G(2d, p) level.

Coupling Constants Calculation. The Monte Carlo search using MMFF method led to 65, 174, 173, and 144 conformers of the four isomers 10*S*, 11*R*/10*R*, 11*S*/10*R*, 11*R*/10*S*, 11*S*, of compound **20** with energy window 30 kJ mol^{-1}. These conformers were preoptimized with HF/3-21G level, and the resulting conformers (<20 kJ mol^{-1}) were reoptimized using MPW1PW91/6-31g(d) basis set in vacuo. In turn, the coupling constants of lower energy conformers (population >1%) were calculated with NMR/GIAO MPW1PW91/6-31g(d, p) method in vacuo, and the final *J* values of each isomer were obtained by averaging the *J* values of conformers with Boltzmann distribution.

Phyllanthacidoid acid methyl ester (1). White amorphous powder: $[\alpha]^{25}_D$ +9.1 (*c* 0.8, MeOH); UV (MeOH) λ_{max} (log ε) 202.0 (4.30), 257.6 (4.22) nm; ECD (in MeOH, λ_{max} [nm],Φ [mdeg]) 237 (−6.7), 263 (−0.4), 281 (−2.0); IR (KBr) ν_{max} 3430, 2960, 1709, 1609, 1276, 1116 cm^{-1}; ^{1}H NMR (CD_3OD, 500 MHz) and ^{13}C NMR (CD_3OD, 125 MHz) data, see Table 2 and Table 1; ESIMS *m/z* 451 [M − H]$^-$; HRESIMS *m/z* 451.1621 [M − H]$^-$ (calcd for $C_{22}H_{27}O_{10}$, 451.1610).

Phyllanthacidoid A (2). Off white amorphous powder: ECD (in MeOH, λ_{max} [nm],Φ [mdeg]) 237 (−6.1), 263 (0.6), 281 (−1.5); ^{1}H NMR (CD_3OD, 600 MHz) and ^{13}C NMR (CD_3OD, 100 MHz) data, see Table 2 and Table 1; ESIMS *m/z* 810 [M + Na]$^+$; HRESIMS *m/z* 810.2805 [M + Na]$^+$ (calcd for $C_{35}H_{49}NNaO_{19}$, 810.2791).

Phyllanthacidoid B (3). Off white amorphous powder: ECD (in MeOH, λ_{max} [nm], Φ [mdeg]) 225 (−6.8), 246 (3.3), 280 (−1.1); ^{1}H NMR (CD_3OD, 600 MHz) and ^{13}C NMR (CD_3OD, 100 MHz) data, see Table 2 and Table 1; ESIMS *m/z* 794 [M + Na]$^+$; HRESIMS *m/z* 794.2841 [M + Na]$^+$ (calcd for $C_{35}H_{49}NNaO_{18}$, 794.2842).

Phyllanthacidoid C (4). White amorphous powder: $[\alpha]^{25}_D$ +20.2 (*c* 1.0, MeOH); UV (MeOH) λ_{max} (log ε) 199.8 (3.97), 229.2 (4.01), 271.8 (2.98) nm; ECD (in MeOH, λ_{max} [nm], Φ [mdeg]) 225 (−7.9), 247 (4.2), 280 (−1.3); IR (KBr) ν_{max} 3430, 2932, 1716, 1279, 1116,

1073 cm^{-1}; ^{1}H NMR (CD_3OD, 500 MHz) and ^{13}C NMR (CD_3OD, 125 MHz) data, see Table 2 and Table 1; ESIMS *m/z* 753 [M + Na]$^+$; HRESIMS *m/z* 775.2652 [M + HCOO]$^-$ (calcd for $C_{34}H_{47}O_{20}$, 775.2666).

Phyllanthacidoid D (5). White amorphous powder: $[\alpha]^{25}_D$ +7.3 (*c* 1.1, MeOH); UV (MeOH) λ_{max} (log ε) 202.0 (4.14), 257.6 (4.06) nm; ECD (in MeOH, λ_{max} [nm], Φ [mdeg]) 235 (−6.7), 262 (1.7), 284 (−1.4); IR (KBr) ν_{max} 3426, 2930, 1689, 1609, 1278, 1116, 1076 cm^{-1}; ^{1}H NMR (CD_3OD, 600 MHz) and ^{13}C NMR (CD_3OD, 150 MHz) data, see Table 2 and Table 1; ESIMS *m/z* 769 [M + Na]$^+$; HRESIMS *m/z* 745.2552 [M − H]$^-$ (calcd for $C_{33}H_{45}O_{19}$, 745.2561).

Phyllanthacidoid E (6). White amorphous powder (purity 80%, estimated from ^{1}H NMR integral): $[\alpha]^{25}_D$ −1.3 (*c* 1.0, MeOH); UV (MeOH) λ_{max} (log ε) 202.8 (3.93), 257.2 (3.83) nm; ECD (in MeOH, λ_{max} [nm], Φ [mdeg]) 237 (−6.9), 263 (−0.3), 279 (−1.8); ^{1}H NMR (DMSO-d_6, 600 MHz) and ^{13}C NMR (DMSO-d_6, 150 MHz) data, see Table 2 and Table 1; ESIMS *m/z* 583 [M − H]$^-$; HRESIMS *m/z* 583.2029 [M − H]$^-$ (calcd for $C_{27}H_{35}O_{14}$, 583.2032).

Phyllanthacidoid F (7). White amorphous powder (purity 90%, estimated from ^{1}H NMR integral): $[\alpha]^{25}_D$ −10.6 (*c* 1.4, MeOH); UV (MeOH) λ_{max} (log ε) 202.2 (4.28), 257.8 (4.18) nm; ECD (in MeOH, λ_{max} [nm], Φ [mdeg]) 237 (−5.1), 263 (0.1), 280 (−1.4); IR (KBr) ν_{max} 3430, 2934, 1610, 1280, 1116, 1075 cm^{-1}; ^{1}H NMR (CD_3OD, 600 MHz) and ^{13}C NMR (CD_3OD, 125 MHz) data, see Table 4 and Table 3; ESIMS *m/z* 802 [M − H]$^-$; HRESIMS *m/z* 802.2770 [M − H]$^-$ (calcd for $C_{35}H_{48}NO_{20}$, 802.2775).

Phyllanthacidoid G (8). White amorphous powder (purity 90%, estimated from ^{1}H NMR integral): $[\alpha]^{25}_D$ −1.0 (*c* 1.1, MeOH); UV (MeOH) λ_{max} (log ε) 202.0 (4.20), 257.8 (4.18) nm; ECD (in MeOH, λ_{max} [nm], Φ [mdeg]) 236 (−6.6), 260 (1.6), 282 (−1.1); IR (KBr) ν_{max} 3426, 2931, 1708, 1609, 1279, 1076 cm^{-1}; ^{1}H NMR (CD_3OD, 400 MHz) and ^{13}C NMR (CD_3OD, 100 MHz) data, see Table 4 and Table 3; ESIMS *m/z* 785 [M + Na]$^+$; HRESIMS *m/z* 761.2507 [M − H]$^-$ (calcd for $C_{33}H_{45}O_{20}$, 761.2510).

Phyllanthacidoid H (9). White amorphous powder (purity 90%, estimated from ^{1}H NMR integral): $[\alpha]^{25}_D$ +9.2 (*c* 0.9, MeOH); UV (MeOH) λ_{max} (log ε) 202.8 (4.18), 257.8 (4.20) nm; ECD (in MeOH, λ_{max} [nm], Φ [mdeg]) 236 (−5.7), 260 (2.6), 282 (−1.1); IR (KBr) ν_{max} 3429, 2926, 1690, 1609, 1280, 1075 cm^{-1}; ^{1}H NMR (CD_3OD, 800 MHz) and ^{13}C NMR (CD_3OD, 100 MHz) data, see Table 4 and Table 3; ESIMS *m/z* 947 [M + Na]$^+$; HRESIMS *m/z* 923.3029 [M − H]$^-$ (calcd for $C_{39}H_{55}O_{25}$, 923.3038).

Phyllanthacidoid I (10). White amorphous powder: $[\alpha]^{25}_D$ +18.0 (*c* 0.9, MeOH); UV (MeOH) λ_{max} (log ε) 202.4 (4.29), 257.6 (4.24) nm; ECD (in MeOH, λ_{max} [nm], Φ [mdeg]) 236 (−6.3), 260 (2.4), 284 (−1.2); IR (KBr) ν_{max} 3429, 2934, 1709, 1609, 1276, 1076 cm^{-1}; ^{1}H NMR (CD_3OD, 500 MHz) and ^{13}C NMR (CD_3OD, 125 MHz) data, see Table 4 and Table 3; ESIMS *m/z* 799 [M + Na]$^+$; HRESIMS *m/z* 775.2660 [M − H]$^-$ (calcd for $C_{34}H_{47}O_{20}$, 775.2666).

Phyllanthacidoid J (11). White amorphous powder: $[\alpha]^{25}_D$ +11.2 (*c* 0.8, MeOH); UV (MeOH) λ_{max} (log ε) 202.2 (4.30), 257.8 (4.20) nm; ECD (in MeOH, λ_{max} [nm], Φ [mdeg]) 235 (−3.4), 263 (0.6), 285 (−1.0); IR (KBr) ν_{max} 3425, 2934, 1610, 1276, 1075 cm^{-1}; ^{1}H NMR (CD_3OD, 600 MHz) and ^{13}C NMR (CD_3OD, 150 MHz) data, see Table 4 and Table 3; ESIMS *m/z* 840 [M + Na]$^+$; HRESIMS *m/z* 816.2910 [M − H]$^-$ (calcd for $C_{36}H_{50}NO_{20}$, 816.2932).

Phyllanthacidoid K (12). White amorphous powder: $[\alpha]^{25}_D$ +12.4 (*c* 1.0, MeOH); UV (MeOH) λ_{max} (log ε) 200.2 (4.04), 228.6 (3.91), 271.8 (2.98) nm; ECD (in MeOH, λ_{max} [nm], Φ [mdeg]) 225 (−4.8), 246 (1.9), 281 (−1.0); IR (KBr) ν_{max} 3425, 2932, 1717, 1643, 1278, 1114, 1073, 1029 cm^{-1}; ^{1}H NMR (CD_3OD, 600 MHz) and ^{13}C NMR (CD_3OD, 100 MHz) data, see Table 5; ESIMS *m/z* 778 [M + Na]$^+$; HRESIMS *m/z* 754.2922 [M − H]$^-$ (calcd for $C_{35}H_{48}NO_{17}$, 754.2928).

Phyllanthacidoid L (13). White amorphous powder: $[\alpha]^{25}_D$ +7.8 (*c* 1.0, MeOH); UV (MeOH) λ_{max} (log ε) 202.6 (4.24), 257.6 (4.17) nm; ECD (in MeOH, λ_{max} [nm], Φ [mdeg]) 236 (−6.5), 261 (−0.03), 280 (−1.8); IR (KBr) ν_{max} 3421, 2934, 1717, 1609, 1277, 1114, 1077, 1031 cm^{-1}; ^{1}H NMR (CD_3OD, 600 MHz) and ^{13}C NMR (CD_3OD, 150 MHz) data, see Table 5; ESIMS *m/z* 794 [M + Na]$^+$; HRESIMS *m/z* 770.2858 [M − H]$^-$ (calcd for $C_{35}H_{48}NO_{18}$, 770.2877).

Phyllanthacidoid M (14). White amorphous powder (purity 80%, estimated from ^{1}H NMR integral): $[\alpha]^{25}_D$ +15.1 (c 0.7, MeOH); UV (MeOH) λ_{max} (log ε) 203.0 (4.27), 257.6 (4.26) nm; ECD (in MeOH, λ_{max} [nm], Φ [mdeg]) 236 (−7.0), 261 (1.3), 282 (−1.6); IR (KBr) ν_{max} 3428, 2933, 1688, 1609, 1277, 1076 cm^{-1}; ^{1}H NMR (CD$_3$OD, 600 MHz) and ^{13}C NMR (CD$_3$OD, 100 MHz) data, see Table 5; ESIMS m/z 753 [M + Na]$^+$; HRESIMS m/z 729.2596 [M − H]$^-$ (calcd for C$_{33}$H$_{45}$O$_{18}$, 729.2611).

Phyllanthacidoid N (15). White amorphous powder: $[\alpha]^{25}_D$ −77.4 (c 0.7, MeOH); UV (MeOH) λ_{max} (log ε) 202.4 (4.27), 258.4 (4.23), 322.8 (3.23) nm; ECD (in MeOH, λ_{max} [nm], Φ [mdeg]) 216 (0.3), 257 (−3.9); IR (KBr) ν_{max} 3427, 2930, 1610, 1280, 1076 cm^{-1}; ^{1}H NMR (CD$_3$OD, 600 MHz) and ^{13}C NMR (CD$_3$OD, 150 MHz) data, see Table 7 and Table 6; ESIMS m/z 810 [M + Na]$^+$; HRESIMS m/z 786.2816 [M − H]$^-$ (calcd for C$_{35}$H$_{48}$NO$_{19}$, 786.2826).

Phyllanthacidoid O (16). White amorphous powder (purity 80%, estimated from ^{1}H NMR integral): $[\alpha]^{25}_D$ −52.6 (c 0.5, MeOH); UV (MeOH) λ_{max} (log ε) 202.6 (4.20), 257.6 (4.20) nm; ECD (in MeOH, λ_{max} [nm], Φ [mdeg]) 215 (−0.1), 245 (−2.4); IR (KBr) ν_{max} 3426, 2924, 1610, 1280, 1076 cm^{-1}; ^{1}H NMR (CD$_3$OD, 600 MHz) and ^{13}C NMR (CD$_3$OD, 150 MHz) data, see Table 7 and Table 6; ESIMS m/z 785 [M + Na]$^+$; HRESIMS m/z 761.2500 [M − H]$^-$ (calcd for C$_{33}$H$_{45}$O$_{20}$, 761.2510).

Phyllanthacidoid P (17). White amorphous powder: $[\alpha]^{25}_D$ −149.7 (c 0.5, MeOH); UV (MeOH) λ_{max} (log ε) 202.6 (4.23), 257.4 (4.20) nm; ECD (in MeOH, λ_{max} [nm], Φ [mdeg]) 226 (−0.4), 258 (−2.5); ^{1}H NMR (CD$_3$OD, 600 MHz) and ^{13}C NMR (CD$_3$OD, 150 MHz) data, see Table 7 and Table 6; HRESIMS m/z 816.2922 [M − H]$^-$ (calcd for C$_{36}$H$_{50}$NO$_{20}$, 816.2932).

Phyllanthacidoid Q (18). White amorphous powder: $[\alpha]^{25}_D$ −38.6 (c 1.1, MeOH); UV (MeOH) λ_{max} (log ε) 202.2 (4.24), 258.4 (4.23) nm; ECD (in MeOH, λ_{max} [nm], Φ [mdeg]) 257 (−4.1), 290 (3.9); IR (KBr) ν_{max} 3431, 2929, 1713, 1609, 1279, 1077 cm^{-1}; ^{1}H NMR (CD$_3$OD, 600 MHz) and ^{13}C NMR (CD$_3$OD, 150 MHz) data, see Table 7 and Table 6; ESIMS m/z 808 [M + Na]$^+$; HRESIMS m/z 784.2647 [M − H]$^-$ (calcd for C$_{35}$H$_{46}$NO$_{19}$, 784.2670).

Phyllanthacidoid R (19). White amorphous powder: $[\alpha]^{25}_D$ −35.7 (c 0.6, MeOH); UV (MeOH) λ_{max} (log ε) 202.8 (4.26), 258.2 (4.26) nm; ECD (in MeOH, λ_{max} [nm], Φ [mdeg]) 257 (−2.8), 290 (2.2); IR (KBr) ν_{max} 3432, 2923, 1713, 1610, 1280, 1072 cm^{-1}; ^{1}H NMR (CD$_3$OD, 600 MHz) and ^{13}C NMR (CD$_3$OD, 150 MHz) data, see Table 7 and Table 6; ESIMS m/z 767 [M + Na]$^+$; HRESIMS m/z 743.2396 [M − H]$^-$ (calcd for C$_{33}$H$_{43}$O$_{19}$, 743.2404).

Phyllanthacidoid S (20). White amorphous powder: $[\alpha]^{25}_D$ −21.7 (c 0.6, MeOH); UV (MeOH) λ_{max} (log ε) 202.6 (4.39), 257.4 (4.24) nm; ECD (in MeOH, λ_{max} [nm], Φ [mdeg]) 234 (−1.5), 264 (−0.5); IR (KBr) ν_{max} 3429, 2923, 1634, 1610, 1278, 1074 cm^{-1}; ^{1}H NMR (CD$_3$OD, 600 MHz) and ^{13}C NMR (CD$_3$OD, 150 MHz) data, see Table 8; ESIMS m/z 826 [M + Na]$^+$; HRESIMS m/z 802.2766 [M − H]$^-$ (calcd for C$_{35}$H$_{48}$NO$_{20}$, 802.2775).

Phyllanthacidoid T (21). White amorphous powder: $[\alpha]^{25}_D$ −11.4 (c 0.8, MeOH); UV (MeOH) λ_{max} (log ε) 202.6 (4.16), 257.4 (4.16) nm; ECD (in MeOH, λ_{max} [nm], Φ [mdeg]) 233 (−1.0), 264 (−0.2); IR (KBr) ν_{max} 3426, 2923, 1713, 1610, 1280, 1072 cm^{-1}; ^{1}H NMR (CD$_3$OD, 600 MHz) and ^{13}C NMR (CD$_3$OD, 150 MHz) data, see Table 8; HRESIMS m/z 761.2500 [M − H]$^-$ (calcd for C$_{33}$H$_{45}$O$_{20}$, 761.2510).

Alkaline Hydrolysis of 2. Compound **2** (40 mg) was added to 2 mL of NaOH solution (0.1 M), and incubated at 50 °C water bath for 30 min. Then the solution was cooled to room temperature and neutralized by Aberlite IR 120. The elution was evaporated to dryness and subjected to silica gel (CHCl$_3$/MeOH/H$_2$O 8:2:0−8:3:0.2) to afford phyllanthacidoid acid (**2a**, 20 mg): white amorphous powder; 1D and 2D NMR spectrum (CH$_3$OD, 600 MHz), see Figure S161−S168 in Supporting Information; ESIMS m/z 437 [M − H]$^-$. *Scyllo* quercitol-2-*O*-β-glucosamine-*N*-acetate (10 mg): white amorphous powder; $[\alpha]^{25}_D$ −16.4 (c 1.2, MeOH); ^{1}H NMR (pyridine-d_5, 600 MHz) δ_H 3.98 (1H, overlap, H-1), 3.92 (1H, dd, J = 9.1, 9.1 Hz, H-2), 4.02 (1H, overlap, H-3), 3.92 (1H, dd, J = 8.9, 8.9 Hz, H-4), 3.98 (1H, overlap, H-5), 2.02 (1H, q, J = 12.0 Hz, H-6a), 2.68 (1H, dt, J = 12.5, 4.4 Hz, H-6b), 5.35 (1H, d, J = 8.6 Hz, H-1′), 4.48 (1H, overlap, H-2′), 4.29 (1H, dd, J = 8.7, 9.7 Hz, H-3′), 4.18

(1H, dd, J = 9.3, 9.3 Hz, H-4′), 3.99 (1H, m, H-5′), 4.53 (1H, dd, J = 2.6, 11.7 Hz, H-6′a), 4.26 (1H, dd, J = 6.5, 11.7 Hz, H-6′b), 2.09 (1H, s, H-2″); ^{13}C NMR (pyridine-d_5, 150 MHz) δ_C 68.7 (C-1), 90.5 (C-2), 75.0 (C-3), 79.2 (C-4), 69.7 (C-5), 38.6 (C-6), 104.4 (C-1′), 58.8 (C-2′), 77.0 (C-3′), 72.1 (C-4′), 78.4 (C-5′), 62.3 (C-6′), 172.2 (C-1″), 23.3 (C-2″); ESIMS m/z 366 [M − H]$^-$; HRESIMS m/z 366.1407 [M − H]$^-$ (calcd for C$_{14}$H$_{24}$NO$_{10}$, 366.1406).

Acid Hydrolysis of 2 and 4. Compounds **2** and **4** (each 20 mg), and 2 mL of HCl solution (3 M), were added respectively to vials and sealed, and then the mixture was incubated in an 80 °C water bath for 3 h. After cooling to room temperature, the mixtures were neutralized by Aberlite IRA-401. The eluates were evaporated to dryness. The products were further purified by silica gel (CHCl$_3$/MeOH/H$_2$O 8:2:0.2−8:3:0.2) to give *scyllo* quercitol and glucosamine from **2**, and *scyllo* quercitol and D-glucose from **4**, respectively. *Scyllo* quercitol: off white amorphous powder; $[\alpha]^{25}_D$ −16.4 (c 1.2, MeOH); ^{1}H NMR (pyridine-d_5, 600 MHz), see Figure S175 in Supporting Information. Glucosamine: off white amorphous powder; $[\alpha]^{25}_D$ +10.6 (c 0.2, MeOH); ESIMS m/z 213 [M + Cl]$^-$. Glucose: off white amorphous powder; $[\alpha]^{25}_D$ +26.6(c 0.6, MeOH); ^{1}H NMR (pyridine-d_5, 600 MHz), see Figure S176 in Supporting Information.

Virus and Cell Culture. HepG2.2.2.15 cells were used for HBV inhibition, which was cultured in MEM (Sigma, St. Louis, USA) supplemented with 10% fetal bovine serum (FBS), 0.03% glutamine, 100 unit/mL penicillin, 100 unit/mL streptomycin, and 100 unit/mL kanamycin. The inhibition to HBsAg and HBeAg was detected by enzyme-linked immunosorbent assay (ELISA) kit (KeHua Inc., China) following the manufacturer's protocol.[22]

Cytotoxicity Assay. HepG2.2.2.15 cells were plated in 96-well plates in 100 μL of medium, which were incubated for 24 h (5% CO$_2$, 37 °C) to form cells monolayers, and the test samples were added at varied concentrations. After 72 h incubation, MTT [[3-(4,5-dimethylthiazol-2-yl)-2,5-diphenyl tetrazolium bromide] solution [0.5 mg mL^{-1} in phosphate buffered saline (PBS)] was added (20 μL per well), and the incubation was continued for another 4 h to give a formazan product. In each well, 200 μL of DMSO was added after the medium was removed, and it was then incubated overnight for the formazan product to dissolve completely. The absorbance of the solution was measured at 490 nm using a Bio-Rad 680 plate reader. Compound concentrations reducing the viability of cells culture by 50% (CC$_{50}$) were calculated by regression analysis of the dose−response curves.

Antivirus Assay. HepG2.2.2.15 cells (100 μL per well) were plated in 96-well plates and incubated for 24 h (5% CO$_2$, 37 °C) to form monolayers. The tested compounds at dose below CC50 (50 μL per well) each with equal volume were added, and the incubation followed for 6 days. The supernatant was collected and stored at −20 °C. ELISA method was applied to detect the contents of HBsAg and HBeAg. IC$_{50}$ values (the concentration of test compounds required to reduce 50% of HBsAg and HBeAg secretion) were calculated according to the regression analysis of the dose−response curves. Lamivudine was tested as the positive control of anti-HBV.

■ ASSOCIATED CONTENT

ⓢ Supporting Information

The ^{1}H and ^{13}C NMR, HSQC, HMBC, HSQC-TOCSY, ^{1}H−^{1}H COSY, ROESY, HETLOC, HRESIMS spectra for compounds **1−21**, and the aglycon (**2a**) and the saccharide of **2**. This material is available free of charge via the Internet at http://pubs.acs.org.

■ AUTHOR INFORMATION

Corresponding Authors

*Tel: +86-871-6522-3235. Fax: +86-871-6522-3235. E-mail: minxu@mail.kib.ac.cn.
*E-mail: zhangyj@mail.kib.ac.cn.

Notes

The authors declare no competing financial interest.

■ REFERENCES

(1) Kupchan, S. M.; LaVoie, E. J.; Branfman, A. R.; Fei, B. Y.; Bright, W. M.; Bryan, R. F. *J. Am. Chem. Soc.* **1977**, *99*, 3199.

(2) Pettit, G. R.; Cragg, G. M.; Gust, D.; Brown, P.; Schmidt, J. M. *Can. J. Chem.* **1982**, *60*, 939.

(3) Pettit, G. R.; Cragg, G. M.; Niven, M. L.; Nassimbeni, L. R. *Can. J. Chem.* **1983**, *61*, 2630.

(4) Pettit, G. R.; Cragg, G. M.; Suffness, M. I.; Gust, D.; Boettner, F. E.; Williams, M.; Saenzrenauld, J. A.; Brown, P.; Schmidt, J. M.; Ellis, P. D. *J. Org. Chem.* **1984**, *49*, 4258.

(5) Pettit, G. R.; Schaufelberger, D. E. *J. Nat. Prod.* **1988**, *51*, 1104.

(6) Pettit, G. R.; Schaufelberger, D. E.; Nieman, R. A.; Dufresne, C.; Saenzrenauld, J. A. *J. Nat. Prod.* **1990**, *53*, 1406.

(7) Zhang, Y. J.; Tanaka, T.; Iwamoto, Y.; Yang, C. R.; Kouno, I. *J. Nat. Prod.* **2000**, *63*, 1507.

(8) Zhang, Y. J.; Tanaka, T.; Iwamoto, Y.; Yang, C. R.; Kouno, I. *Tetrahedron Lett.* **2000**, *41*, 1781.

(9) Zhang, Y. J.; Tanaka, T.; Iwamoto, Y.; Yang, C. R.; Kouno, I. *J. Nat. Prod.* **2001**, *64*, 870.

(10) Liu, Q.; Wang, Y. F.; Chen, R. J.; Zhang, M. Y.; Yang, C. R.; Zhang, Y. J. *J. Nat. Prod.* **2009**, *72*, 969.

(11) Vongvanich, N.; Kittakoop, P.; Kramyu, J.; Tanticharoen, M.; Thebtaranonth, Y. *J. Org. Chem.* **2000**, *65*, 5420.

(12) Liu, M.; Xiao, H.-T.; He, H.-p.; Hao, X.-Y. *Chem. Nat. Compd.* **2008**, *44*, 588.

(13) Xiao, H. T.; He, H. P.; Peng, J.; Wang, Y. H.; Yang, X. W.; Hu, X. J.; Hao, X. Y.; Hao, X. J. *J. Asian. Nat. Prod. Res.* **2008**, *10*, 1.

(14) Smith, A. B.; Hale, K. J.; Vaccaro, H. A.; Rivero, R. A. *J. Am. Chem. Soc.* **1991**, *113*, 2112.

(15) Matsumori, N.; Kaneno, D.; Murata, M.; Nakamura, H.; Tachibana, K. *J. Org. Chem.* **1999**, *64*, 866.

(16) Plaza, A.; Bifulco, G.; Keffer, J. L.; Lloyd, J. R.; Baker, H. L.; Bewley, C. A. *J. Org. Chem.* **2008**, *74*, 504.

(17) Mailliard, M. E.; Gollan, J. L. *Annu. Rev. Med.* **2006**, *57*, 155.

(18) Dougherty, A. M.; Guo, H.; Westby, G.; Liu, Y.; Simsek, E.; Guo, J. T.; Mehta, A.; Norton, P.; Gu, B.; Block, T.; Cuconati, A. *Antimicrob. Agents Chemother.* **2007**, *51*, 4427.

(19) Yu, W.; Goddard, C.; Clearfield, E.; Mills, C.; Xiao, T.; Guo, H.; Morrey, J. D.; Motter, N. E.; Zhao, K.; Block, T. M.; Cuconati, A.; Xu, X. *J. Med. Chem.* **2011**, *54*, 5660.

(20) Shin, M. S.; Kang, E. H.; Lee, Y. I. *Antiviral Res.* **2005**, *67*, 163.

(21) Frisch, M. J.; Trucks, G. W.; Schlegel, H. B.; Scuseria, G. E.; Robb, M. A.; Cheeseman, J. R.; Scalmani, G.; Barone, V.; Mennucci, B.; Petersson, G. A.; Nakatsuji, H.; Caricato, M.; Li, X.; Hratchian, H. P.; Izmaylov, A. F.; Bloino, J.; Zheng, G.; Sonnenberg, J. L.; Hada, M.; Ehara, M.; Toyota, K.; Fukuda, R.; Hasegawa, J.; Ishida, M.; Nakajima, T.; Honda, Y.; Kitao, O.; Nakai, H.; Vreven, T.; Montgomery, J. A.; Peralta, J. E.; Ogliaro, F.; Bearpark, M.; Heyd, J. J.; Brothers, E.; Kudin, K. N.; Staroverov, V. N.; Kobayashi, R.; Normand, J.; Raghavachari, K.; Rendell, A.; Burant, J. C.; Iyengar, S. S.; Tomasi, J.; Cossi, M.; Rega, N.; Millam, J. M.; Klene, M.; Knox, J. E.; Cross, J. B.; Bakken, V.; Adamo, C.; Jaramillo, J.; Gomperts, R.; Stratmann, R. E.; Yazev, O.; Austin, A. J.; Cammi, R.; Pomelli, C.; Ochterski, J. W.; Martin, R. L.; Morokuma, K.; Zakrzewsk, V. G.; Voth, G. A.; Salvador, P.; Dannenberg, J. J.; Dapprich, S.; Daniels, A. D.; Farkas, O.; Foresman, J. B.; Ortiz, J. V.; Cioslowski, J.; Fox, D. J. *Gaussian 09*, Revision A.02; Gaussian, Inc.: Wallingford, CT, 2009.

(22) Li, J.; Huang, H.; Feng, M.; Zhou, W.; Shi, X.; Zhou, P. *Antiviral Res.* **2008**, *79*, 114.